1970

Applications of heat pipes to nuclear reactor engineering

Monte Bryce Parker
Iowa State University

APPLICATIONS OF HEAT PIPES TO NUCLEAR REACTOR ENGINEERING

by

Monte Bryce Parker

A Dissertation Submitted to the
Graduate Faculty in Partial Fulfillment of
The Requirements for the Degree of
DOCTOR OF PHILOSOPHY

Major Subject: Nuclear Engineering

Approved:

Signature was redacted for privacy.

In Charge of Major Work

Signature was redacted for privacy.

Head of Major Department

Signature was redacted for privacy.

Dean of Graduate College

Iowa State University
Of Science and Technology
Ames, Iowa

1970

TABLE OF CONTENTS

I. INTRODUCTION

The heat pipe is a device normally used to obtain a comparatively high transfer of thermal energy. It consists of a containment vessel (the pipe), a wicking material, and a fluid in two phases. The most common geometry is that shown schematically in Figure 1.

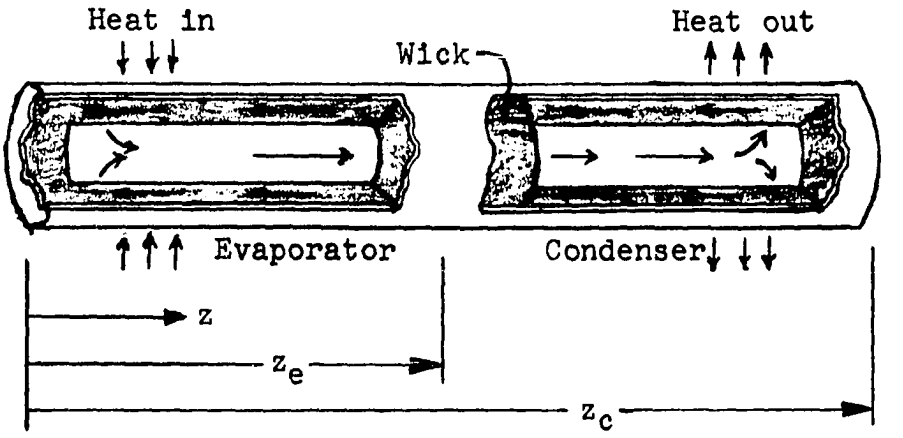

Figure 1. Heat Pipe

It consists of a long narrow tube which forms a closed outer shell. The wick is a porous material which is in firm contact with the inside wall of the tube. The liquid phase of the fluid is in the wick and vapor phase is in the core or center of the tube.

The heat pipe works in the following manner. Heat is added to the evaporator end of the heat pipe. This causes liquid contained in the wick of the evaporator end to vaporize and results in a slight pressure drop in the vapor phase

from the evaporator to condenser. Vapor then flows to the condenser end where it condenses on the wick. The evaporation of liquid in the evaporator section causes tiny meniscii to form on the wick surface. These support a pressure drop between the liquid and vapor phases of the evaporator section, liquid flows through the wick from the condenser to the evaporator and completes the cycle.

There is a wide variety of working fluids depending on the function and temperature of operation of the heat pipe. The working fluid is chosen so that its normal boiling temperature is somewhat below the temperature of operation. This temperature can vary from the cryogenic range to any upper range that can be tolerated by the containment.

Wick structures also vary widely in design depending on the use. They can be made from any porous material, or from channels machined in the wall. These channels can be uncovered or covered with screen. The wick structure can also be merely an annular space with a fine mesh screen separating the liquid and vapor phases with the liquid flowing down the annular space.

Heat pipes have been used in many applications where high thermal energy transfer is needed or constant temperature or heat flux is desired. This includes such things as cooling devices for electronic components, heat exchangers, and temperature control devices. Although they have been used

to some extent in radioisotope (12) power sources, their application for cooling reactors is only in the preliminary design stages (2, 11, 27).

A new concept involving the use of heat pipes as control devices for nuclear reactors will be investigated in this thesis. The feature of the concept is that the heat pipe will contain a fissionable material as the working fluid. The primary purpose of the heat pipe will be to change the amount of fuel within a reactor instead of the usual purpose of transferring heat.

This change in the amount of fuel results because of the relationship of the heat transferred in the heat pipe to the amount of liquid in the evaporator section. Chapter III gives a description of the system used for this study which is a model based on the nuclear rocket engines used in a Nerva rocket. In Chapter IV, the equations to determine this relationship are derived.

II. REVIEW OF THE LITERATURE

The use of heat pipes as heat transfer mechanisms has been a relatively recent development. In 1964, Grover (15) et al. at Los Alamos published the results of the first experimental work done with heat pipes. Since that time the interest in heat pipes has grown greatly with theoretical and experimental work being done at many other facilities (1, 5). However, most work was and still is done at Los Alamos (10). In 1965, Cotter (8, 9) published the first comprehensive theoretical treatment of steady state heat pipe operation following with a theoretical treatment of startup dynamics in 1967.

Kemme (19, 20, 21) and his associates at Los Alamos have done much of the experimental work with high performance heat pipes. The results from his work are especially useful for high temperatures and liquid metals.

Hampel and Koopman (16) have given a theoretical treatment of some of the mass changes taking place in an operating heat pipe for a number of liquid metal systems. Although their results fail to take into account some important parameters, they are useful for studying reactivity changes for cases of solid fuels cooled by heat pipes with liquid metal fluid.

Cheung (6) has published a comprehensive general review

of heat pipe theory and applications up through the middle of 1968 and Feldman and Whiting (13, 14) have presented a review of many novel applications.

The theoretical study of rocket reactor control has been presented by Smith (30), Smith and Stenning (31), Jansen and Buckner (18), and Mohler and Perry (28).

III. OBJECT OF INVESTIGATION

This thesis is a feasibility study of the use of heat pipes containing liquid fissionable material as control devices for a nuclear reactor.

The reactor model which will be used is based on a nuclear rocket reactor such as Nerva. The heat pipes are inserted into the reactor as shown in Figure 2. The evaporator end of the heat pipe projects into the end of the reactor where the hydrogen gas leaves the reactor and enters the rocket chamber. The H_2 is used to cool the reactor and propel the rocket. The condenser end of the heat pipe will be in the chamber where it will be cooled by the exiting H_2 gas.

The working liquid of the heat pipe is UF_4. The UF_4 will fission in the evaporator end causing the heat pipe to circulate UF_4 vapor from evaporator to condenser and liquid UF_4 from the condenser to evaporator in the normal fashion of a heat pipe.

The heat pipe will affect the reactivity because the amount of UF_4 in the evaporator will vary with the heat flux and temperature of operation.

Instead of a wick of porous material, an annular channel for liquid flow with a fine mesh screen separating the two phases as shown in Figure 3 will be used. This type of liquid return channel was chosen because of the function of

this heat pipe. The heat will be generated within the liquid channel and it is therefore not necessary to have as good thermal conduction between the fluid and containment wall as channels would provide. It is also necessary to have a screen because a variation in the amount of fluid in the evaporator section of the heat pipe will be due to the change in the depth of the meniscus within each screen opening. This meniscus is illustrated in Figure 4 where r_s is the radius of the screen opening which has been approximated with a circle. This type of wick has been tested experimentally by Kemme (19) and has high performance characteristics. The reason for this is it allows easier flow of liquid than would be allowed by using a porous material for the wick.

The reactor has a nominal power of 1000 MW. The core is graphite with UC dispersed throughout. The concentration of the fuel is varied so that a constant flux in the radial direction is achieved. It has a beryllium reflector on the radial sides and there is some reflection on the top due to the dense, cold entering H_2. There is assumed to be no reflection on the lower end where the H_2 exists due to its low density of the gas. There is no reason to try to flatten the axial flux and it will be assumed to be one-half of a chopped cosine from the center to the exit end as shown by Cooper (7). The maximum flux at nominal power is 2×10^{15} n/cm^2 sec.

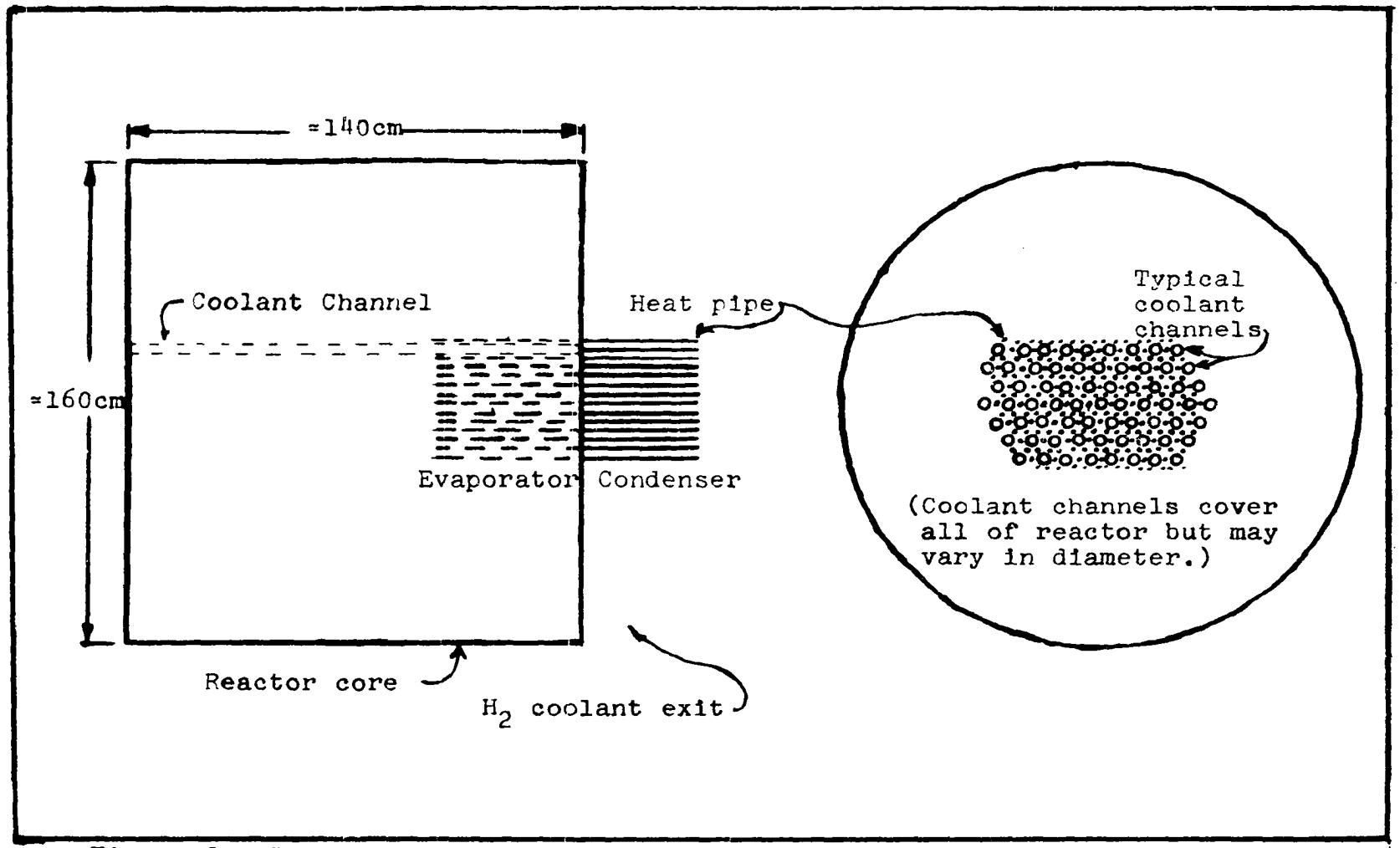

Figure 2. Reactor core with heat pipe

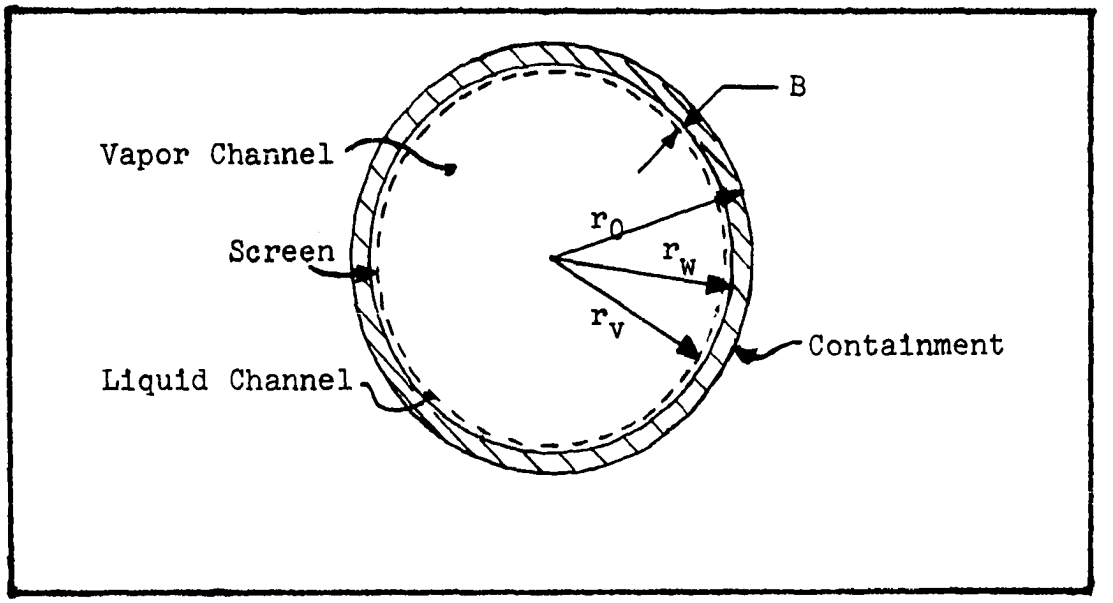

Figure 3. Heat pipe cross-section

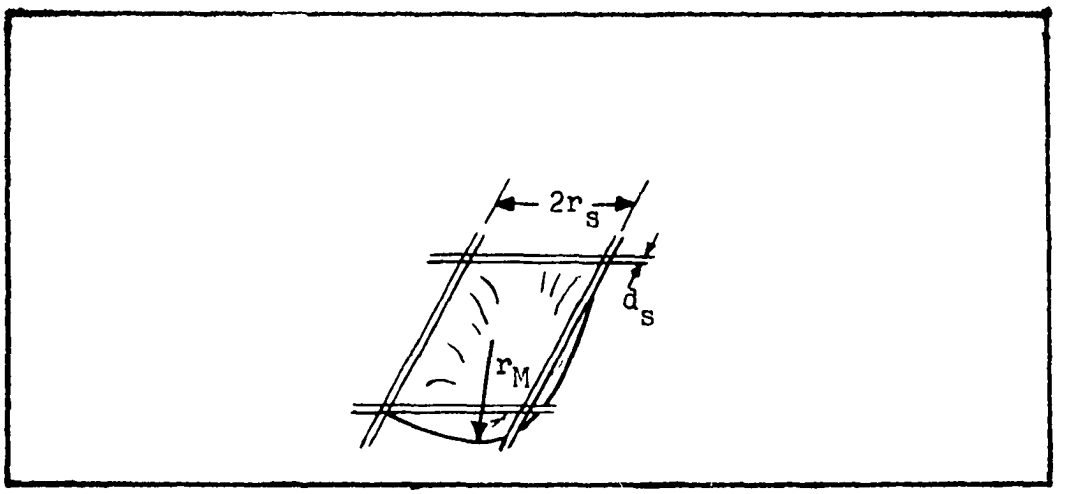

Figure 4. Meniscus in screen opening

The reactor size is approximately 3.0 m^3 with a 33% void fraction due to the cylindrical coolant channels. The arrangement of the heat pipes in the reactor is shown in Figure 2 and the total number of the heat pipes will be used as a parameter.

There were a number of reasons for using this type of system. The reason for choosing UF_4 is that it is one of the few stable compounds of uranium which is a liquid at low enough temperatures and on which there is sufficient data on its properties. UF_4 is stable at elevated temperatures and will react very little with graphite (35). Another compound which would possibly work is UCl_4 with a normal boiling point of 792°C. However, very limited data are available on the properties of this compound.

The reason for using a reactor model design based on a rocket reactor is that this heat pipe must be at very high temperatures. The normal boiling point of UF_4 is 1723°K and efficient operation of the heat pipe dictates that a high temperature reactor be used. The nominal exit temperature of the H_2 is chosen to be 2200°K.

In the following section the equations will be derived which can be used to determine the relationship between the neutron flux, temperature, and reactivity change due to one heat pipe at the radial center of the reactor. A perturbation analysis will be used to relate mass changes and

reactivity. More heat pipes can then be added to increase the reactivity.

The total time dependent operation of the reactor will then be analyzed including major feedback processes. An analog computer will be used to solve this section of the problem.

IV. THEORY

In this chapter the equations are derived which are necessary to relate the reactivity changes caused by the heat pipe to the liquid mass changes in the evaporator section of the heat pipe. The neutron kinetics of the reactor are then analyzed in order to see how the heat pipes affect the feedback of the system.

A theoretical treatment of heat pipes was first published by Cotter (9) where he used the pressure drops within the heat pipe to determine some of the heat transfer properties of the heat pipe. He assumed constant heat fluxes at both evaporator and condenser. His wick was a porous material as compared to the annular channel used here, and he did not have the thermal energy produced within the heat pipe.

The approach used by Cotter will be used for the initial part of this derivation except that most of the terms will be different because of the difference in the heat pipes and application.

In order to determine the mass changes within the heat pipe, it is necessary to relate the fluid flow to the heat generation within the heat pipe. This is done by looking at the conservation of energy along a streamline. The approach that will be used is to add the pressure drops around a closed circuit along a streamline within the heat pipe.

The pressure drops will be due to four processes. 1)

Pressure drop due to liquid flow, 2) to vapor flow, 3) to surface tension effects, 4) and to evaporation and condensation. From this, an expression for the radii of the meniscii can be derived leading to an expression for mass changes.

The following format will be used to determine reactivity effects. The pressure drop terms will be derived in terms of the total heat flow Q(z). Q(z) will then be related to heat generation rate and dimensions of heat pipes. The resulting equations will be used to determine an expression for $r_M(Z)$. The mass of the fuel displaced by the meniscus is found from r_M and the reactivity due to this mass is determined. The temperature effects are then derived and related to the heat flux and fluid properties. Finally, the reactivity of other feedback mechanisms is added to the reactivity of the heat pipe.

It will be assumed for the following derivations that steady state conditions exist.

A. Derivation of $r_M(z)$

1. Liquid pressure gradient

The liquid flows from the condenser to the evaporator along an annular space between the inside wall of the heat pipe and the screen. Since the distance between the inside wall and the screen is small compared to the radius of the heat pipe, the liquid flow can be approximated as flow between

two parallel planes. Poiseuille's Law plus a gravity term can be used for the pressure drop in the liquid if laminar flow is assumed.

$$\frac{dp_l}{dz} = - \frac{12\mu_l \bar{V}}{B^2} + \rho_l g \sin \theta \qquad (1)$$

The average velocity, $\bar{V}$,* is equal to the total mass flow rate divided by the flow area and liquid density.

$$\bar{V} = \frac{\dot{m}_l}{2\pi r_v B \rho_l} \qquad (2)$$

This gives the pressure drop in terms of the mass flow rate

$$\frac{dp_l}{dz} = - \frac{6\mu_l \dot{m}_l}{\pi r_v B^3 \rho_l} + \rho_l g \sin \theta \qquad (3)$$

The total liquid mass flow past a point along the heat pipe must equal the total vapor mass flow in the other direction under steady state conditions. The heat carried by the vapor at a position z' results from vaporization of liquid in the evaporator between z=o and z=z'. The total heat carried by the vapor at z is then

$$Q(z) = H_v \dot{m}_v(z) \qquad (4)$$

and since $\dot{m}_v(z) = \dot{m}_l(z)$,

$$Q(z) = - H_v \dot{m}_l(z) \qquad (5)$$

---

* A list of symbols is given in section IX, page 78.

The liquid pressure drop can now be written in terms of Q(z).

$$\frac{dp_l}{dz} = \frac{6\mu_l Q(z)}{\pi r_v B^3 H_v \rho_l} + \rho_l g \sin\theta \qquad (6)$$

2. Vapor pressure gradient

The pressure drop in the vapor is harder to determine. This is because the velocity in the radial direction cannot be ignored as it was in the liquid case.

Knight and McInteer (24) have published a theoretical treatment of flow in channels with porous walls as have Yuan and Finkelstein (38). Wageman and Guevara (36) have determined experimentally the flow characteristics for laminar flow in a cylindrical pipe with injection and suction through the wall.

If the radial Reynolds number defined by $Re_r = \frac{\rho_v r_v \bar{V}_{vr}}{\mu_v} = -\frac{1}{2\pi r}\frac{d\dot{m}_v}{dz}$ is large, ie. $Re_r >> 1$ then the pressure drop for this type of flow can be approximated by the following equation.

$$\frac{dp_v}{dz} = -\frac{am_v}{4\rho_v r_v^4}\frac{d\dot{m}_v}{dz} \qquad (7)$$

where $a = 1$ for evaporation and $a = \frac{4}{\pi^2}$ for condensation.

The pressure drop in the vapor of the heat pipe will be assumed to behave in the same manner as flow described by the preceding authors (24, 36, 38). The pressure drop in the

vapor phase in the heat pipe can be written in terms of Q(z) as

$$\frac{dp_v}{dz} = - \frac{aQ(z)}{4\rho_v r_v^4 H_v^2} \frac{dQ(z)}{dz} \tag{8}$$

3. Meniscus pressure drop

The pressure drop between the liquid and vapor at any value of z due to the liquid meniscus is

$$\Delta p_M(z) = \frac{2\gamma}{r_M(z)} \tag{9}$$

where r_M is the radius of the meniscus as shown in Figure 4. This result is based on the assumption that the meniscus can be approximated by the section of a sphere.

4. Pressure drop due to evaporation and condensation

There will also be pressure drop between liquid and vapor at any given z location due to the actual evaporation or condensation process.

The rate at which gas molecules strike a given area of an enclosure can be derived from gas kinetics (29).

$$\frac{dm_v^*}{dt} = \rho v \left(\frac{RT}{2\pi M}\right)^{1/2} \tag{10}$$

where m_v^* is the mass of gas striking the given area. For the case of the inside of the heat pipe tube,

$$dm_v^*(z) = 2\pi r_v \rho_v \left(\frac{RT_v}{2\pi M}\right)^{1/2} dz \tag{11}$$

is the rate the gas molecules strike a differential area of length dz. If ideal gas behavior is assumed,

$$\rho_v = \frac{p_v \overline{M}}{RT} \tag{12}$$

This relationship is inserted into Equation 11, which is then divided by dz.

$$\frac{d\dot{m}_v^*}{dz} = \frac{2\pi r_v p_v \overline{M}}{RT_v}\left(\frac{RT_v}{2\pi\overline{M}}\right)^{1/2} = \frac{r_v p_v}{\left(\frac{RT}{2\pi\overline{M}}\right)^{1/2}} \tag{13}$$

The rate at which the gas molecules would leave the liquid due to evaporation is

$$\frac{d\dot{m}_v^*}{dz} = \frac{r_v p_{vp}}{\left(\frac{RT_v}{2\pi\overline{M}}\right)^{1/2}} \tag{14}$$

where p_{vp} is the vapor pressure of the liquid.

The assumption is made that the probability for evaporation and condensation of molecules passing through the surface is approximately one. The mass flow rate of the vapor is

$$\frac{\dot{dm}_v}{dz} = \frac{r_v}{\left(\frac{RT_v}{2\pi\overline{M}}\right)^{1/2}} (p_v - p_{vp}) \tag{15}$$

Q(z) is substituted into Equation 15 and it is solved for the pressure drop at z due to evaporation or condensation

$$\Delta p_e = \frac{\left(\frac{RT_v}{2\pi\overline{M}}\right)^{1/2}}{r_v H_v} \frac{dQ(z)}{dz} \tag{16}$$

5. Evaluation of Q(z)

In order to evaluate the pressure drop it is necessary to relate Q(z), the total heat carried by the vapor at point z, to the heat flux density generated in the evaporator by fissioning. The generation of heat per unit volume will be designated by $q'''(z)$ and is a function of z. This heat generation will take place in the annular region where the liquid exists if it is assumed that the heat generated in the vapor can be ignored. The heat will flow to the liquid vapor interface where it will be carried away by the vaporization of the liquid.

Under steady state conditions the following heat equation can be written for the system.

$$k\nabla^2 T(r, z) + q'''(z) = 0 \qquad (17)$$

The rate of change of temperature in the z direction is very small compared to that in the r direction and can be neglected. This means that ∇^2 can be replaced by $\left(\frac{d^2}{dr^2} + \frac{1}{r}\frac{d}{dr}\right)$. Equation 17 becomes,

$$k\frac{d^2T}{dr^2} + k\frac{1}{r}\frac{dT}{dr} + q'''(z) = 0 \qquad (18)$$

By integrating this expression once and recognizing that $q'''(z)$ is not a function of r,

$$\frac{dT}{dr} = -\frac{q'''(z)}{k}\frac{r}{2} + \frac{C_1}{r} \qquad (19)$$

where C_1 is a constant of integration. Let $q''(r, z)$ be the

radial heat flux and assume that this is negligible at the outer surface of the evaporator section of the heat pipe. This is a good assumption since the heat pipe and the surrounding medium are designed to be at nearly the same temperature and most of the heat generated in the heat pipe goes into vaporizing the liquid.

This condition will give the following boundary condition,

$$q''(r_w, z) = - k_1 \left.\frac{dt}{dr}\right|_{r_w} = 0 \tag{20}$$

From this, C_1 can be evaluated.

$$C_1 = \frac{q''(z)}{2} \frac{r_w^2}{k_1} \tag{21}$$

The total heat carried by the vapor is

$$Q(z) = - \int_o^z 2\pi r_v q''(r_v, z)\, dz$$

$$= \pi r_v^2 \left[\frac{r_w^2}{r_v} - 1\right] \int_o^z q'''(z)\, dz \tag{22}$$

The substitution $r_w = r_v + B$ is made yielding,

$$Q(z) = \pi r_v^2 \left[\left(1 + \frac{B}{r_v}\right)^2 - 1\right] \int_o^z q'''(z)\, dz \tag{23}$$

Since $q'''(z)$ will be proportional to the neutron flux, it could be approximated by a portion of a cosine curve. There is little reflection of the flux at the end of the reactor

where the heat pipes are located.

The value of $q'''(z)$ is,

$$q'''(z) = q_o \cos \frac{\pi(z + z_b)}{2z_1} \tag{24}$$

where q_o would be the value of $q'''(z)$ at the position of maximum flux if the heat pipe went into the reactor that far. z_b is the distance from the point of maximum flux to the beginning of the heat pipe and z_1 is the distance from the position of maximum flux to the position where the flux goes to zero. This will be a short distance outside the reactor.

The value of $Q(z)$ in the evaporator can now be found.

$$Q_e(z) = \pi r_v^2 q_o \left[\left(1 + \frac{B}{r_v}\right)^2 - 1\right] \int_o^z \cos \frac{\pi(z' + z_b)}{2z_1} \, dz'$$

$$= 2z_1 r_v^2 q_o \left[\left(1 + \frac{B}{r_v}\right)^2 - 1\right] \left[\sin \frac{\pi(z+z_b)}{2z_1} - \sin \frac{\pi z_b}{2z_1}\right] \tag{25}$$

and

$$\frac{dQ_e(z)}{dz} = \pi r_v^2 q_o \left[\left(1 + \frac{B}{r_v}\right)^2 - 1\right] \left[\cos \frac{\pi(z+z_b)}{2z_1}\right] \tag{26}$$

In the condenser section, it will be assumed that heat is removed uniformly through the heat pipe wall to the hydrogen gas. Therefore, in the condenser, $q_c''(r, z) = \text{constant}$.

The total heat entering the condenser is equal to the heat leaving the evaporator. Since this heat is removed uniformly,

$$\frac{Q_c(z)}{Q(z_e)} = \frac{2r_v(z_c - z)\, q''_c}{2r_v(z_c - z_e)q''_{cc}}$$

$$Q_c(z) = Q(z_e)\, \frac{(z_c - z)}{(z_c - z_e)} \tag{27}$$

$Q(z_e)$ can be obtained by use of Equation 25. On inserting this into Equation 27, the total heat flow in the condenser at any location z is given.

$$Q_c(z) = 2z_1 r_v^2 q_o \left[\left(1 + \frac{B}{r_v}\right)^2 - 1 \right]$$

$$x\left[\sin \frac{\pi(z_e + z_b)}{2z_1} - \sin \frac{\pi z_b}{2z_1}\right]\left[\frac{z_c - z}{z_c - z_e}\right] \tag{28}$$

$$\frac{dQ_c(z)}{dz} = - \frac{2z_1 r_v^2 q_o}{(z_c - z_e)} \left[\left(1 + \frac{B}{r_v}\right)^2 - 1\right]\left[\sin \frac{\pi(z_e + z_b)}{2z_1} - \sin \frac{\pi z_b}{2z_1}\right] \tag{29}$$

6. Pressure drop in liquid and vapor

Now that Q(z) is known, the expressions involving spatial derivatives of pressure may be integrated. Since it is desired to find r_M as a function of z in the evaporator, the total pressure drop around the heat pipe will be found from an arbitrary z in the evaporator down to the end of the condenser where $r_M = \infty$ and back to the position z. In one direction the circuit will go through the vapor and in the other direction through the liquid.

The total pressure drop in the vapor phase of the condenser can be obtained by inserting Equation 25 and 26 into

Equation 8 and integrating from $z = z_e$ to $z = z_c$.

$$\int_{z_e}^{z_c} \frac{dp_v}{dz}\, dz = p_v(z_c) - p_v(z_e) = \frac{4A^2}{\pi^2 \rho_v (z_c - z_e)^2}$$

$$x \left[\sin \frac{\pi(z_e + z_b)}{2z_1} - \sin \frac{\pi z_b}{2z_1} \right]^2 \int_{z_e}^{z_c} (z_c - z)\, dz \qquad (30)$$

where

$$A = q_o z_1 \frac{\left[\left(1 + \frac{B}{r_v} \right)^2 - 1 \right]}{H_v} \qquad (31)$$

By carrying out the integration,

$$p_v(z_v) - p_v(z_e) = \frac{2A^2}{\pi^2 \rho_v} \left[\sin \frac{\pi(z_e + z_b)}{2z_1} - \sin \frac{\pi z_b}{2z_1} \right] \qquad (32)$$

It might be noted in passing that the pressure drop in the vapor phase in the condenser is not dependent on the condenser length $(z_c - z_e)$ nor on the radius of the heat pipe r_v except in the term $\left[\left(1 + \frac{B}{r_v} \right)^2 - 1 \right]$.

The vapor pressure drop in the evaporator is found in an analogous manner. Integration is carried out from z to z_e.

$$p_v(z_e) - p_v(z) = -\frac{A^2}{2\rho_v} \left[\left(\sin \frac{\pi(z_e + z_b)}{2z_1} - \sin \frac{\pi z_b}{2z_1} \right)^2 - \left(\sin \frac{\pi(z + z_b)}{2z_1} - \sin \frac{\pi z_b}{2z_1} \right)^2 \right] \qquad (33)$$

In order to get the total pressure drop in the liquid phase in the condenser and evaporator, Equation 6 is used. For the condenser,

$$\int_{z_e}^{z_c} \frac{dp_l}{dz}\, dz = p_l(z_c) - p_l(z_e) =$$

$$\frac{6\mu_l}{\pi r_v B^3 H_v \rho_l} \int_{z_e}^{z_c} Q_c(z)dz + \rho_l g(z_c - z_e) \sin\theta$$

$$= \frac{6\mu_l}{\pi B^3 \rho_l} Ar_v \left[\sin \frac{\pi(z_e + z_b)}{2z_l} - \sin \frac{\pi z_b}{2z_l}\right]\left[z_c - z_e\right]$$

$$\rho_l g(z_c - z_e) \sin\theta \qquad (34)$$

and for the evaporator,

$$p_l(z_e) - p_l(z) = \frac{12\mu_l}{\pi B^3 \rho_l} Ar_v \left[-\frac{2z_l}{\pi}\left(\cos \frac{\pi(z_e+z_b)}{2z_l}\right.\right.$$

$$\left.\left. - \cos \frac{\pi(z+z_b)}{2z_l}\right) - (z_e - z) \sin \frac{\pi z_b}{2z_l}\right] + \rho_l g(z_e - z) \sin\theta \qquad (35)$$

7. Final equation for $r_M(z)$

The sum of the pressure drops around the heat pipe can now be expressed. For an arbitrary position z in the evaporator,

$$\Delta p_M(z) + \Delta p_e(z) + p_v(z_c) - p_v(z) + \Delta p_M(z_c)$$

$$+ \Delta p_e(z_c) + p_l(z) - p_l(z_c) = 0. \qquad (36)$$

$p_M(z_c)$ is approximately zero since $r_M \simeq \infty$ at $z = z_c$.

$\left[p_v(z_c) - p_v(z)\right]$ is obtained from Equations 32 and 33 and the fact that $\left[p_v(z_c) - p_v(z)\right] = \left[p_v(z_c) - p_v(z_e)\right] + \left[p_v(z_e) - p_v(z)\right]$. Likewise, $\left[p_l(z) - p_l(z_c)\right]$ is obtained using Equations 34 and 35.

On substituting the values for the pressure terms into Equation 36, the following equation results.

$$\frac{2\gamma}{r_M(z)} - \frac{A^2}{2\rho_v}\left[S_1^2 - S_2^2(z) - \frac{4}{\pi^2}S_1^2\right]$$

$$- \frac{6\mu_l Ar_v}{\rho_l B^3 \pi}\left[\frac{4z_l}{\pi}S_3(z) - 2(z_e - z)\sin\frac{\pi z_b}{2z_l} + (z_c - z_e)S_1\right] \qquad (37)$$

$$-\rho_l g (z_c - z)\sin\theta - \sqrt{\frac{RT}{2\pi M}}\,Ar_v\left[\frac{\pi}{z_l}\cos\frac{\pi(z+z_b)}{2z_l} + \frac{2S_1}{(z_c - z_e)}\right] = 0$$

where

$$S_1 = \sin\frac{\pi(z_e+z_b)}{2z_l} - \sin\frac{\pi z_b}{2z_l}$$

$$S_2(z) = \sin\frac{\pi(z+z_b)}{2z_l} - \sin\frac{\pi z_b}{2z_l}$$

$$S_3(z) = \cos\frac{\pi(z+z_b)}{2z_l} - \cos\frac{\pi(z_e+z_b)}{2z_l}$$

Equation 37 can now be used to solve for the dimensionless quantity $r_v/r_M(z)$. The result is

$$\frac{r_v}{r_M(z)} = \frac{1}{4}\left[\frac{A^2 r_v}{\rho_v \gamma}\right]\left[\left(1 - \frac{4}{\pi^2}\right) S_1^2 - S_2^2(z)\right] + 3\left[\frac{A r_v \mu_1 z_1}{B^3 \rho_1 \gamma}\right]$$

$$\left[\frac{4}{\pi} S_3(z) - 2\frac{(z_e - z)}{z_1} \sin\frac{\pi z_b}{2z_1} + \frac{(z_c - z_e)}{z_1} S_1\right] + \left[\frac{\rho_1 g r_v (z_c - z)}{2} \sin\theta\right]$$

$$+ \left[\frac{A r_v^2}{z_1 \gamma}\sqrt{\frac{RT}{2\pi M}}\right]\left[\frac{\pi}{2}\cos\frac{\pi(z+z_b)}{2z_1} + \frac{z_1}{(z_c - z_e)} S_1\right]. \qquad (38)$$

The quantities in brackets are dimensionless.

Equation 38 is used to solve for $r_M(z)$ as a function of q_o, temperature, and any variations in dimensions that are made. Most of the variation in temperature is through the change in the properties of UF_4.

B. Evaluation of M and $\frac{d\Delta M(z)}{dz}$

Once $r_M(z)$ is known, the change in the amount of fuel in the evaporator can be determined. Figure 4 shows a schematic drawing of the wire mesh which separates the liquid and vapor phase.

The area of the square between wires is approximated with a circle of radius r_s. The volume of liquid removed by the meniscus can be approximated (33) by

$$V_M(z) = \frac{2}{3}\pi r_M^3\left[1 - \left(1 - \frac{3}{4}\left(\frac{r_s}{r_M}\right)^4 - \frac{1}{4}\left(\frac{r_s}{r_M}\right)^6\right)^{1/2}\right] \qquad (39)$$

It would be exactly this if the square were a circle.

The number of meniscii around the circumference of the pipe at any location, z, is

$$N_c = \frac{2\pi r_v}{(2r_s+d_s)}$$

where d_s is the wire diameter. The fraction of the mass of the liquid that is removed by the meniscus per meniscus length in the z direction is approximately equal to $\frac{d\Delta M(z)}{dz}$.

$$\frac{d\Delta M(z)}{dz} = \frac{\rho_l V_M(z) N_c}{(2r_s+d_s)} = \rho_l V_M(z) \frac{2\pi r_v}{(2r_s+d_s)^2} \tag{40}$$

The total mass removed in the evaporator due to all the meniscii is

$$\Delta M = \int_0^{z_e} \frac{d\Delta M(z)}{dz} dz \tag{41}$$

C. Derivation of Heat Pipe Effect On Reactivity

A perturbation technique is used to determine the effect on reactivity of small changes of fuel in the evaporator of the heat pipe. The analysis is carried out on one heat pipe located along the axial center of the reactor. At this position, it is assumed that one group perturbation theory can be used. This approximation should be reasonable since the heat pipe is located far from the reflectors. It is also assumed that a small change in the amount of fuel will change

the macroscopic fission and capture cross-sections but will not change the diffusion coefficient. The perturbation analysis is based on the technique used by Lamarsh (25).

From the results of a one group perturbation analysis, the reactivity can be written as (26)

$$\frac{\Delta k}{k} = \delta_{HP} = \frac{\int_V (\nu \delta\Sigma_f - \delta\Sigma_a)\phi^2(z)dV}{\nu \int_V \Sigma_f \phi^2(z)dV} \tag{42}$$

$\delta\Sigma_f$ and $\delta\Sigma_a$ are functions of the change in $\frac{d\Delta M(z)}{dz}$ which will be denoted as $\delta\Delta M(z)$. They are zero outside the volume of $\Delta M(z)$. For this reason, the volume integral in the numerator of Equation 42 can be changed to an integral over the length of the heat pipe evaporator. $\delta\Sigma_f$ and $\delta\Sigma_a$ are considered to vary only in the z directions and are not functions of r. They are defined by the following equations.

$$\delta\Sigma_f(z) = \frac{N_a}{\overline{M}_{UF_4}} \sigma_f^{235} \xi \frac{\delta\Delta M(z)}{\int r dr} \tag{43}$$

$$\delta\Sigma_a(z) = \frac{N_a}{\overline{M}} \left[\sigma_a^{235} \xi + \sigma_a^{238} (1 - \xi) \frac{\delta\Delta M(z)}{\int r dr} \right] \tag{44}$$

N_a is Avogadro's Number and ξ is the enrichment. $\int r\, dr$ is an arbitrary constant depending on the limits chosen. Since ϕ varies little in the radial direction and the heat pipe is located at the center of the reactor, ϕ in the numerator of Equation 42 may also be considered to be a function of z only. It is now possible to write Equation 42 in the

following form.

$$\delta_{HP} = \frac{\frac{N_a}{\bar{M}} \int_o^{z_e} [\nu\sigma_f^{235}\xi - \sigma_a^{235}\xi - \sigma^{238}(1-\xi)]\,\delta\Delta M(z)\phi^2(z)dz}{\nu \int_V \Sigma_f \phi^2 dV} \qquad (45)$$

The denominator of the preceding equation is a constant and can be evaluated in the following manner. The square of the flux in this term is approximated by $\phi^2 = \bar{\phi}\phi$, where $\bar{\phi}$ is the average flux in the reactor. The denominator can then be written as

$$\nu\bar{\phi} \int_V \Sigma_f \phi dV. \qquad (46)$$

The integral term is proportional to the power produced in the reactor.

$$\nu\bar{\phi} \int_V \Sigma_f \phi dV = \nu\bar{\phi} eP \qquad (47)$$

P is the reactor power and e is a term relating energy produced per fission per second to power in watts. The flux term in the numerator is a chopped cosine in the area where the heat pipe is located. It is $\phi^2 = \phi_o^2 \cos^2 \frac{\pi(z+z_b)}{2z_1}$, where ϕ_o is the maximum flux in the reactor.

Equation 45 can now be written in the form

$$\delta_{HP} = \frac{N_a \xi \sigma_f^{235} C_2(\xi) \phi_o^2}{\bar{M} e P \bar{\phi}} \int_o^{z_e} \delta\Delta M(z) \cos^2 \frac{\pi(z+z_b)}{2z_1} dz \qquad (48)$$

where $C_2(\xi) = 1 - \frac{\sigma_a^{235}}{\nu\sigma_f^{235}} - \frac{\sigma_a^{235}}{\nu\xi\sigma_f^{235}}(1-\xi)$. The value of

q_o may be substituted into Equation 45. It is

$$q_o = \frac{N_a \rho_1 \xi \sigma_f^{235} \phi_o}{\overline{Me}} \tag{49}$$

This results in the following expression for reactivity.

$$\delta_{HP} = \frac{C_2(\xi) q_o}{\rho_1 p} \frac{\phi_o}{\bar{\phi}} \int_o^{z_e} \delta\Delta M(z) \cos^2 \frac{\pi(z+z_b)}{2z_1} dz \tag{50}$$

The quantity $\frac{q_o}{\rho_1 p}$ depends only on the enrichment and σ_f^{235}. It is not dependent on temperature since σ_f^{235} varies very little with temperature in an intermediate reactor. The quantity $\frac{\phi_o}{\bar{\phi}}$ is constant. It is, therefore, possible to define a new variable

$$C_2(\sigma_f, \xi) = \frac{C_1(\xi) q_o}{\rho_1 p} \frac{\phi_o}{\bar{\phi}} \tag{51}$$

which gives the result

$$\delta_{HP} = C_2(\sigma_f, \xi) \int_o^{z_e} \delta\Delta M(z) \cos^2 \frac{\pi(z+z_b)}{2z_1} dz \tag{52}$$

It is now possible to calculate the reactivity at a given temperature by first choosing an enrichment. q_o is then used in the calculation of $C_2(\sigma_f, \xi)$ and $\frac{d\Delta M(z)}{dz}$. A small change is then made in the flux which results in a small change in q_o and a value for $\delta\Delta M(z)$. The integration is carried out on z and a value for δ_{HP} is determined.

After $\Delta M(z)$ is determined for a given position the amount of fuel at this position changes which causes the radial heat flux to change. An iteration scheme is used to calculate a new A based on an effective change in B. B is changed in the following manner. A new variable B' is defined as the length that B would be reduced at a position z in order for the amount of liquid to decrease by the amount $V_M(z)$.

$$B'(z) = V_M(z)/(2r_M+d_s)^2 \tag{53}$$

A new value of B is determined by the expression

$$B_2(z) = B_1(z) - B'(z) \tag{54}$$

A new value of A is then calculated and from this a new value of $V_M(z)$ is determined. The iteration is continued until B(z) does not change.

D. Temperature Dependence

The next step is to determine how temperature relates to the operation of the heat pipe. A heat pipe is basically an isothermal device since it operates at the temperature at which the liquid and vapor are in equilibrium at a given vapor pressure. There will be a slight drop in temperature and pressure between the evaporator and condenser. Cotter (9) gives some experimental values for a horizontal sodium heat pipe of $\Delta p = 0.5$ mm Hg and $\Delta T = 0.7°K$ for the pressure and

temperature differences in the vapor from one end to the other. The temperature of operation was 920°K so that the temperature drop is a very small fraction of the total temperature. It will therefore be assumed that the temperature is the same for all points in the heat pipe for the following analysis.

1. Temperature and heat flow rate dependence

The temperature of operation of the heat pipe depends on the relationship between the heat production within the heat pipe and the loss through the condenser. The transfer of heat through the condenser wall for steady state conditions is determined using the relationship

$$\frac{1}{r}\frac{d}{dr}\left(r\frac{dT}{dr}\right)=0. \tag{55}$$

This expression is integrated twice using the boundary conditions $q''(r_w) = -k\left.\frac{dT}{dr}\right|_{r=r_w} = \frac{Q(z_e)}{2\pi r_w(z_c-z_e)}$ and $T(r_w) = T_v$.

The temperature at the outside of the heat pipe condenser is then obtained by evaluating the result of the integration at $r = r_o$ where r_o is the outside radius of the heat pipe.

$$T_o = T_v - \frac{Q(z_e)}{2\pi(z_c-z_e)k_G}\ln\frac{r_o}{r_w} \tag{56}$$

$Q(z_e)$ is given by Equation 25 evaluated at $z = z_e$.

Let h be the heat transfer coefficient for transfer of heat from the outside wall of the heat pipe to the hydrogen

gas. By adding a term to include convection to Equation 56, the temperature of the inside of the heat pipe can be related to the exit temperature of the hydrogen.

$$T_v = T_G + \frac{Q(z_e)}{2\pi(z_c - z_e)}\left[\frac{\ln \frac{r_o}{r_w}}{k_G} + \frac{1}{r_o h}\right] \tag{57}$$

By inserting the expression for $Q(z_e)$ from Equation 25, and the dimensions of the heat pipe, the temperature of the heat pipe is determined for a hydrogen gas temperature and heat flux density.

This is again an iteration process because h and k_T are temperature dependent and all of the properties of the heat pipe fluid which are necessary to determine $Q(z_e)$ are temperature dependent.

Equation 58 is used to determine h. This equation which gives the Nusselt Number in terms of the Reynold's Number and Prandtl Number is often used for correlations with high temperature gases.

$$Nu = 0.023\, Re^{0.8}\, Pr^{0.4} \tag{58}$$

These terms are temperature dependent and it is again necessary to use an iteration technique since, for this equation, the properties must be evaluated at the mean temperature of the gas and heat pipe surface.

2. Temperature dependence of properties

In order to evaluate the previously derived parameters, it is necessary to determine the values of heat pipe fluid properties, especially their temperature dependence. Many of the high temperature properties of UF_4 are difficult to determine and approximations are necessary in some cases. The properties which must be evaluated are ρ_l, p_e, p_v, μ_l, and H_v.

The evaluation of p_v is made by determining the vapor pressure at a given temperature and using the ideal gas law. Langer and Blankenship (26) have published an empirical expression for the vapor pressure of UF_4 based on experimental work they did. The expression is

$$\log_{10} P = - 20058/T - 7.05 \log_{10} T + 38.011 \qquad (59)$$

where P has dimensions of mm Hg and T is in degrees Kelvin. These authors also calculated a value of heat of vaporization of $H_v = 51.2 \frac{k\ cal}{mole}$ which is $765 \frac{joules}{gm}$ for UF_4.

There are no experimental data available for the surface tension of UF_4 at the temperatures under consideration. Moore (29) gives an empirical relationship for surface tension which is good for most liquids.

$$\gamma\left(\frac{M}{\rho}\right)^{2/3} = a - bT \qquad (60)$$

"a" and "b" are constants depending on the liquid. Kirshenbaum and Grosse (23) have determined experimentally the

surface tension of UF_4 in the 1309 - 1723°K range. An empirical equation which is good in this range is

$$\gamma = 447.3 - 0.1922\ T \frac{\text{dynes}}{\text{cm}} \tag{61}$$

where T is in degrees Kelvin. Equation 62 based on Equations 60 and 61 will be used here.

$$\gamma = \rho_l^{2/3} \left[131.2 - 0.0564\ T\right] \frac{\text{dynes}}{\text{cm}} \tag{62}$$

ρ_l has units of $^{gm}/_{cm^3}$ and T has units of degrees Kelvin.

The temperature dependence of ρ_l is taken from work published by Kirshenbaum and Cahill (22). The equation used is

$$\rho_l = 7.784 - 9.92 \times 10^{-4}\ T(°K) \frac{\text{gm}}{\text{cm}^3} \tag{63}$$

Experimental values of μ_l could not be found for the temperatures of interest. It was, therefore, necessary to use an analytical approach. The following derivation is based on that suggested by Bird et al. (3), who proved that the viscosity of a liquid can be represented by the relationship

$$\mu_l = \frac{Na\ h_p}{\bar{V}}\ e^{\Delta\bar{G}_o/RT} \tag{64}$$

where h_p is Boltzman's Constant, $\bar{V}$ the volume of one mole of liquid, and $\Delta\bar{G}_o$ is the molar "free energy of activation". $\Delta\bar{G}_o$ is constant for a given fluid and is found empirically to be related to the internal energy of evaporation.

$$\Delta\bar{G}_v \approx 0.408\ \Delta\bar{U}_{VAP} \tag{65}$$

The internal energy of evaporation can be related to the energy of vaporization at the normal boiling point.

$$\Delta\bar{U}_{VAP} \approx \bar{H}_v - RT_b \tag{66}$$

where T_b is the normal boiling point.

On combining Equations 64, 65, and 66 and inserting values appropriate for UF_4, the viscosity is

$$\mu_l = 1.27 \times 10^{-5} \rho_l e^{9810/T} \frac{gm}{cm\ sec} \tag{67}$$

with ρ_l in $\frac{gm}{cm^3}$ and T in °K.

The temperature dependent properties of the hydrogen gas are also necessary. These properties are the thermal conductivity, viscosity, and Prandtl Number and were obtained from "Property Values of Parahydrogen" by M. E. Stephenson (34). These values are needed for the evaluation of Equation 58 which can be written in the following form

$$h = \frac{(0.023)G^{0.8}}{(2r_w)^{0.2}} \frac{k_h}{(\mu_h)^{.8}} Pr_h^{0.4} \tag{68}$$

Where G is the flow rate of hydrogen past the heat pipe.

The only temperature dependent parameter which still must be obtained is the thermal conductivity of the graphite. The equation used for this is

$$k_G = 460/T(°K) + 0.28 \frac{watts}{cm\ °K} \tag{69}$$

This equation is good up to temperatures of 2700°C and is taken from data by Wagner and Dauelsberg (37).

E. Other Reactivity Effects

The time dependent variation of the flux including feedback effects must now be considered in order to determine the overall effect that the heat pipes have on the system. Figure 5 is a schematic drawing of the nuclear rocket engine with the hydrogen coolant flow diagram.

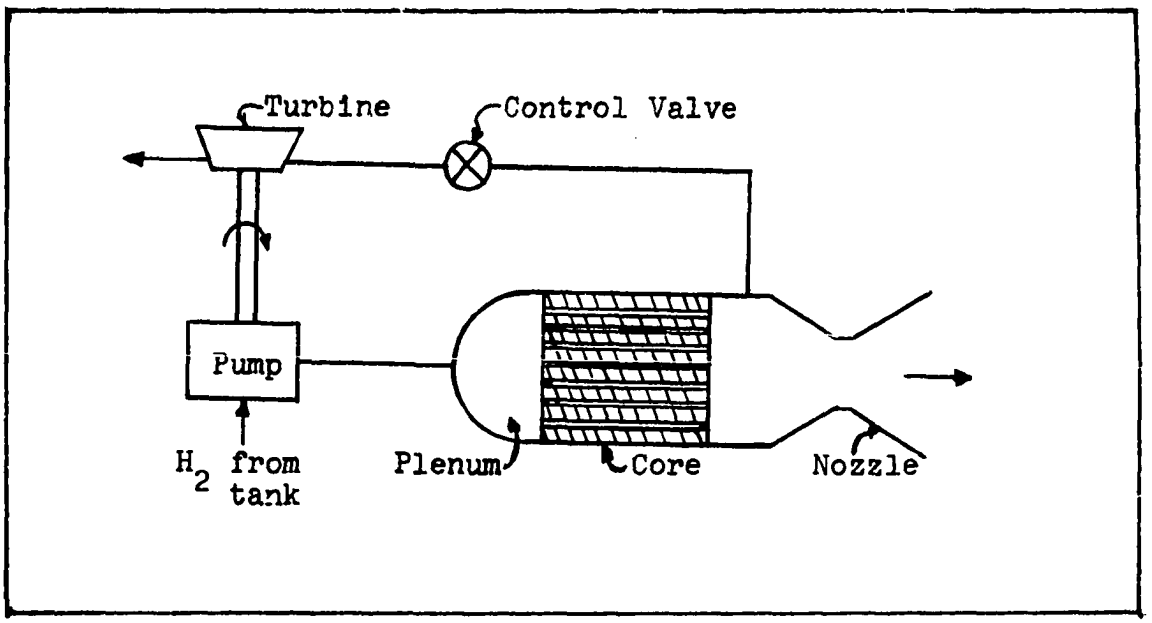

Figure 5. Schematic Drawing of Rocket Engine

A lumped parameter model based in part by that proposed by Smith and Stenning (31) is used to describe the reactor dynamics. For the reactor core, a power balance can be represented by the following equation where radiative heat transfer is neglected.

$$M_r C_r = an - \omega c_p (T_2 - T_1) \tag{70}$$

The subscripts r, 1, and 2 refer to the reactor as a whole, the entrance plenum, and the exit respectively.

If the core power density distribution is assumed constant, the maximum wall surface temperature of the coolant channels is equal to T_2 times a function of $\frac{4fL}{D}$ where f is the function factor, L is the core length, and D the coolant channel diameter. For a lumped parameter model, if $T_{wall\ max}/T_2$ is constant then T_r/T_2 is constant. Equation 70 can then be written as

$$M_r C_r \frac{T_r}{T_2} \frac{dT_2}{dt} = an - \omega c_p T_2 \tag{71}$$

where T_1 is negligible compared to T_2.

The following variables are now defined so that the equation can be put in dimensionless form and referenced to the design values.

$$T = \frac{M_r C_r T_r}{a C_p T_{2d}}$$

$$T' = T_2/T_{2d}$$

$$\omega' = \omega/\omega_d$$

$$n' = an/\omega_d c_p T_{2d} = \frac{n}{n_d} \tag{72}$$

where the subscript d refers to steady state design values.

If the nozzle behind the reactor is choked, then $\omega\sqrt{T_2}/P_2$ and P_2/P_1 are constant. The quantity $\omega' T_2'$ can then be replaced by the quantity $P_1' \sqrt{T_2'}$. Equation 71 can now be written as

$$\tau_T \frac{dT_2'}{dt} = n' - P_1' \sqrt{T_2'} \tag{73}$$

τ_T is approximately 2.5 seconds for the reactor considered in this thesis.

The expression for P_1' involves the behavior of the turbomachinery. The results derived by Smith and Stenning (31) will be used here. These results can be expressed by the equation

$$\tau_p \frac{dP_1'}{dt} = P_1' \sqrt{T_2'} - \frac{(P_1')^2}{T_2'} \tag{74}$$

where τ_p is approximately 12.5 seconds.

The usual neutron kinetics and precursor equations are also needed. These are

$$\frac{dn}{dt} = \frac{\delta-\beta}{\Lambda} n + \sum_{c=1}^{N} \lambda_i C_i \tag{75}$$

$$\frac{dC_i}{dt} = \frac{\beta_i n}{\Lambda} - \lambda_i C_i \tag{76}$$

In terms of dimensionless variables they can be written as,

$$\tau_n \frac{dn'}{dt} = \left(\frac{\delta}{\beta} - 1\right) n' + \sum_{c=1}^{N} \frac{\beta_i}{\beta} C_i' \tag{77}$$

$$\tau_{C_i} \frac{dC_i}{dt} = n' - C_i' \tag{78}$$

where $\tau_n = \frac{\Lambda}{\beta}$ and $\tau_C = \frac{1}{\lambda_i}$.

There will be some time lapse in the heat pipe between the time that the flux increases and the time it takes for the mass change to take place. This can be represented by the equation

$$\tau_Q \frac{dQ'}{dt} = n' - Q' \tag{79}$$

where Q' is a dimensionless number Q/Q_d which represents the change in heat transfer of the heat pipe. τ_Q will be the sum of the time it takes the heat to move from the liquid phase to the vapor phase and the time it takes for it to move from the evaporator to the condenser. If the first of these processes is ignored, then

$$\tau_Q = \frac{\frac{z_c+z_e}{2}}{\bar{V}_v} \tag{80}$$

where $\bar{V}_v$ is the average velocity of the vapor.

$$\bar{V}_v = \frac{\bar{\dot{m}}_v}{\rho_v \pi r_v^2} \; ; \quad \bar{\dot{m}}_v = \frac{\bar{Q}_d}{H_v} \tag{81}$$

The average Q_d will be approximated as the total heat flow at the end of the evaporator. Therefore,

$$\tau_Q = \frac{(z_c+z_e)\rho_v \pi r_v^2 H_v}{2Q(z_e)} \tag{82}$$

It will be seen in the result section that τ_Q has very little effect on the results so that the approximations made in its determination are justified.

The effect of all these parameters on the reactivity of the reactor must now be determined. There are two major processes which affect the reactivity of a reactor of this type besides any external devices such as control rods. The first of these is the increase in reactivity with an increase in the density of hydrogen within the core. This results because the reactor operates with neutrons in the epithermal range and the addition of hydrogen increases moderation and therefore increases the rate of fissioning.

The second effect is due to temperature changes in the graphite which change the diffusion length of the neutrons.

Calculations done by Smith and Stenning (31) indicate that the first effect results in a linear increase in reactivity with hydrogen density and the second effect results in a linear decrease in reactivity with an increase in the square root of the temperature.

Without the heat pipes, the reactivity of the system can be written as

$$\delta = \delta_c + \alpha_p \frac{P_1}{T_2} - \alpha_T \sqrt{T_2} \tag{83}$$

where α_p and α_T are the proportionality constants for the hydrogen density effect and the temperature effect respectively. Equation 83 is non-dimensionalized by making use of steady state values as was previously done

$$\delta' = \delta_c' + \alpha_p' \frac{P_1'}{T_2'} - \alpha_T' \sqrt{T_2'} \tag{84}$$

where

$$\delta' = \delta/\beta$$

$$\delta_c' = \delta_c/\beta$$

$$\alpha_p' = \frac{\alpha_p T_{2d}}{\beta P_{1d}}$$

$$\alpha_T' = \frac{\alpha_T \sqrt{T_{2d}}}{\beta} \tag{85}$$

F. Total Feedback Effects

The introduction of the heat pipes will add another term to the reactivity equation which will be a function of temperature and heat flow, Q, within the heat pipe. The following equation can now be written to describe the control of the reactor.

$$\tau_n \frac{dn'}{dt} - \delta' n' - n' + \sum_{c=1}^{N} \frac{\beta_i}{\beta} C_i \tag{86}$$

$$\tau_{C_i} \frac{dC_i}{dt} = n' - C_i' \tag{87}$$

$$\tau_T \frac{dT_2^1}{dt} = n' - P_1^1 \sqrt{T_2'} \tag{88}$$

$$\tau_p \frac{dP_1'}{dt} = P_1' \sqrt{T_2'} - \frac{(P_1')^2}{T_2'} \tag{89}$$

$$\tau_Q \frac{dQ'}{dt} = n' - Q' \tag{90}$$

$$\delta' = \delta_c' + \alpha_p' \frac{P_1'}{T_2'} - \alpha_T T_2' + f(Q, T_2) \tag{91}$$

$$f(Q, T_2) = \delta_{HP}'$$

V. RESULTS AND DISCUSSION

A digital computer was used to determine the effect that the heat pipes had on the reactivity of the reactor making use of the equations derived in the previous section. After the function $f(Q, T_2)$ was found an analog computer was used to solve equations 86 through 91 and to determine if heat pipes could be used as control mechanisms.

Calculations are performed in the following manner.

A value of flux is chosen. The design value of the flux is $2 \times 10^{15} \frac{n}{cm^2 sec}$ at a rated power of 1000 MW. A value of $\xi\sigma_f^{235}$ is then chosen. The σ_f^{235} as used here is the value averaged over the energy range of the neutrons. It is used mainly as a proportionality constant between neutron density and fissioning rate. Since this is an intermediate reactor, the value of σ_f^{235} will probably be in the range of 50 to 100 barns. However, the product $\xi\sigma_f^{235}$ will be used here so that any variations in σ_f^{235}, which would be determined experimentally, can be accounted for by using UF_4 in the heat pipe of a different ξ. The ratio of $\sigma_a^{235}/\sigma_f^{235}$ and $\sigma_a^{238}/\sigma_f^{235}$ are less dependent on the energy spectrum of the neutrons. Values of these ratios were determined by using the average values in the intermediate groups 10 through 14 of Table 7-2 in ANL-5800. A value of σ_f^{235} of

68 barns is used in the term $\frac{\sigma_a^{238}}{\xi\sigma_f^{235}}$ of $C_2(\xi)$.

It is now necessary to choose a value of T_2. A design value of 2200°K has been chosen for this reactor. This number is based on some of the previously designed rocket reactors and is a little low for some of those in the planning stage (32). By knowing the design power and temperature, the flow rate of the H_2 can be determined. The value of the flow rate is determined from Figure 3-33 in "Fundamentals of Nuclear Flight" by Bussard and DeLauer (4). This figure gives a plot of the ratio of power to flow rate vs. exit gas temperature. This graph agrees very closely with experimental design values given by Spence (32) for reactors of different powers. The design value of flow rate for this reactor is $\omega_d = 30 \frac{kg}{sec}$.

After T_2 is determined, q_o is derived by use of Equation 49 with T_2 used in finding such variables as ρ_1. Once q_o is determined, T_v is determined from Equation 57 and with the iteration mentioned concerning h and k_T. Once T_v is determined it is used to obtain new property values and a new q_o is obtained. This process is repeated until there is no change in q_o. This value of q_o is then used to determine "A" along with the iteration mentioned on page 30. The last derived value of T_v is used for all temperature dependent properties and with chosen dimension, Equations 38 through 40

are used to determine $\frac{d\Delta M}{dz}$. A small change is now made in the flux. This is usually on the order of $\Delta\phi/\phi \quad 5x10^{-4}$. This new flux $\phi_1 = \phi+\Delta\phi$ is then used to find a new $\frac{d\Delta M(z)}{dz}$ and the above process is repeated to determine $\delta\Delta M$ for use in Equation 52. It is then possible to determine $\delta'_{HP}=f(\phi, T_2)$ from this equation.

In order to separate the effects due to changes in flux from those due to changes in T_2, δ_{HP} was obtained at various fluxes with T_2 held constant. The flux was then held constant and δ_{HP} was obtained at different values of T_2. This could be thought of as using different values of ω_d. T_v is still dependent on both q_o and T_2 so that all temperature iterations are still necessary.

Before this process is carried out it is necessary to determine the best values to use for $\xi\sigma_f^{235}$, r_s, z_e, z_c, r_v and B. Most of these terms either have optimum values or have constraints. However, some of them can take on almost any value and not change the results to a large degree. The following section will describe how the values of the variables were arrived at. In all cases, the value of θ was taken as zero.

The value of r_v was chosen to be 0.5 cm strictly on the basis of the space available for the heat pipe. It is an arbitrary selection and increasing it would increase the reactivity change caused by one heat pipe, but would reduce the

number of heat pipes which could be used.

Figures 6 and 7 show the variation in r_M and $\frac{d\Delta M(z)}{dz}$ respectively along the heat pipe evaporator with r_s as a parameter. The different values of r_s do not have much effect on the r_M values but do have a significant effect on ΔM. The problem with going to larger values of r_s which would give a larger ΔM is that the heat pipe loses its ability to pump liquid back to the evaporator with capillary action and it also can burnout when $r_M \to r_s$. When this condition is reached all the liquid will leave the evaporator. This condition is harder to realize than it first appears since as r_M gets smaller, there is less fuel for fissioning which helps retard any further decrease in r_M. That is why the curves for r_M vs. z on Figure 6 are different for different r_s. The larger r_s causes less fuel to be in the evaporator and therefore causes a larger r_M. However, the difference $r_s - r_M(max)$ decreases as r_s increases. This effect is also very dependent on the value of B chosen since this determines the fraction of fuel removed. The design value chosen for r_s is $r_s = 0.02$ cm.

There is usually an optimum value for B for the greatest mass changes. This is due to the fact that smaller B's increase resistance to liquid flow resulting in poorer heat pipe performance but also increase the fraction of fuel removed for a given flux change which gives better performance.

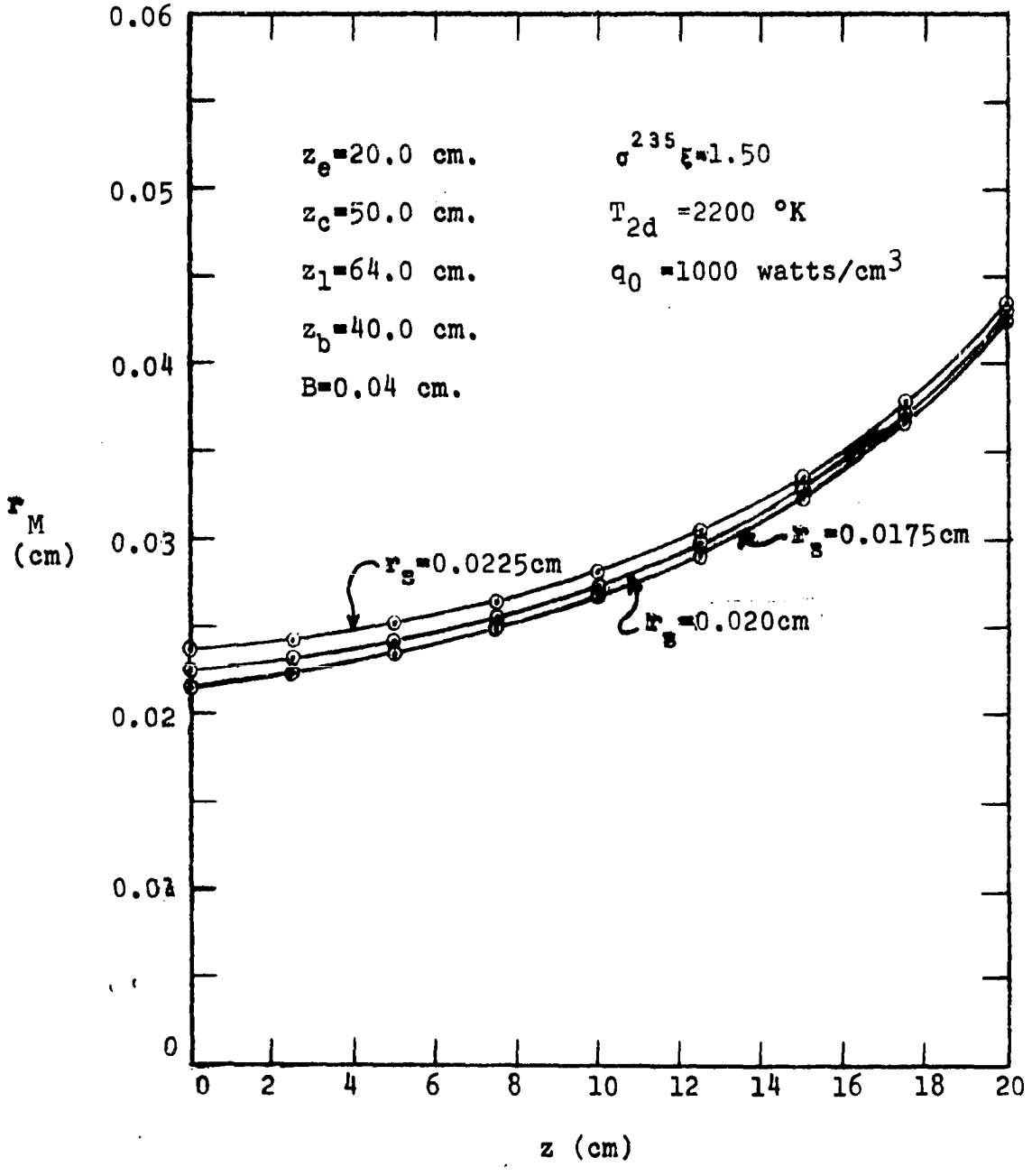

Figure 6. Radius of meniscus vs. distance along evaporator

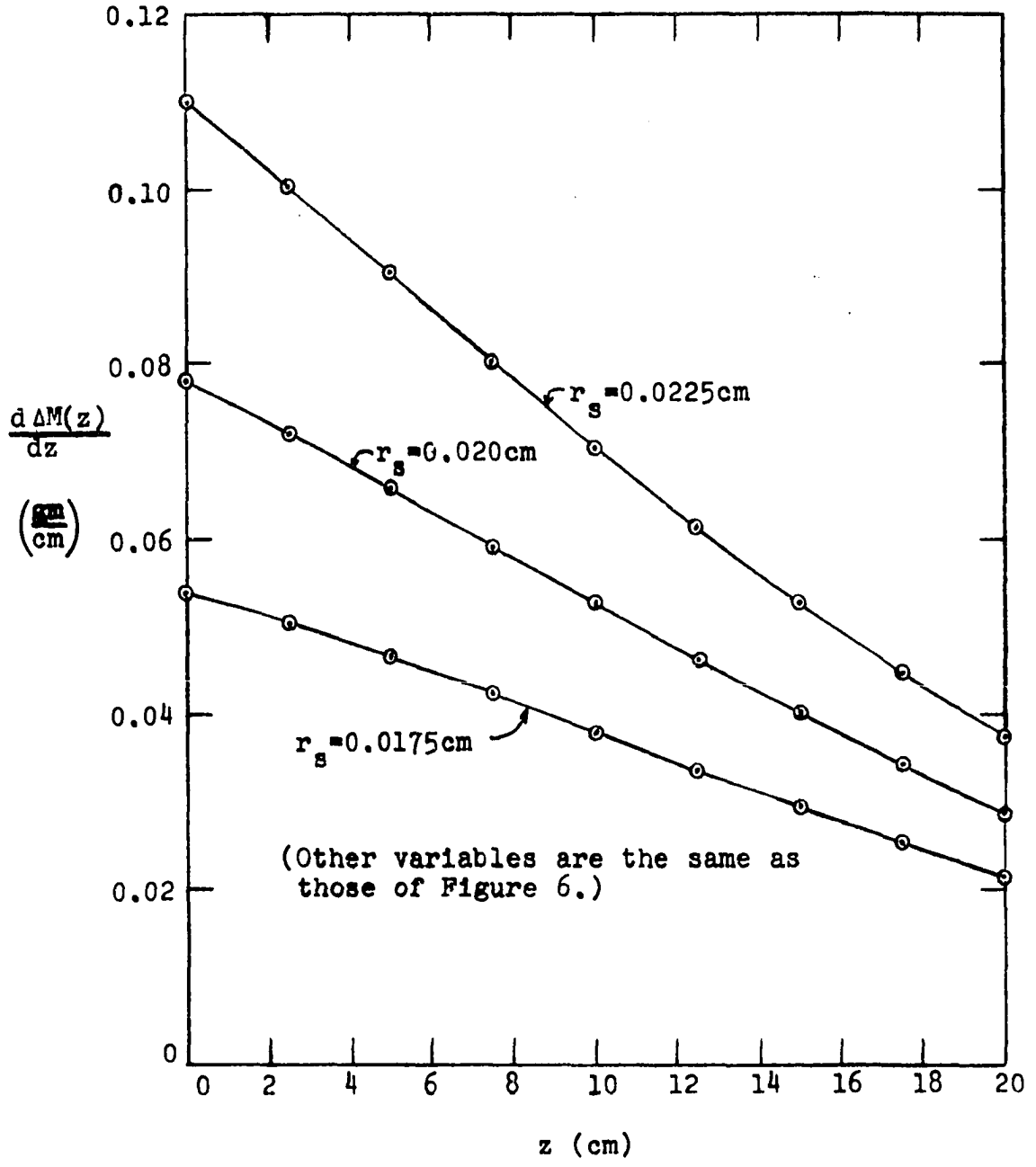

Figure 7. Rate of change of liquid mass along evaporator length vs. evaporator length

Figure 8 is a plot of the maximum value of r_M vs. B. A maximum occurs in this plot which gives the best value of B. The reason this is best is that for all other variables constant, the larger value of r_M allows the use of a larger value of $\xi\sigma_f^{235}$ which increases the reactivity control of the heat pipe. The design value chosen for B is B = 0.04 cm.

Another variable that has an optimum value is the length of the condenser section. The pressure drop due to liquid motion decreases with a decrease in this dimension but the pressure drop due to condensation of liquid increases. The pressure drop due to gravity will depend on orientation if the heat pipe is in a gravity field. Figure 9 shows a relationship between maximum r_M and (Z_c-Z_e).

The choice of Z_e also involves judgment based on conflicting mechanisms. The total mass change in the reactor is increased with an increase in Z_e. But the maximum r_M decreases rapidly with increasing Z_e which means that burnout conditions are approached faster and a smaller value of $\xi\sigma_f^{235}$ must be used which decreases reactivity changes. This has much the same effect that changes in r_s have. Also, having large values of Z_e greatly alters the effect that the heat pipe has on the core such as creating a larger void fraction and causing less moderation. This would make the perturbation analyses result in greater error.

The design value chosen for Z_e and (Z_c-Z_e) are 20 cm and

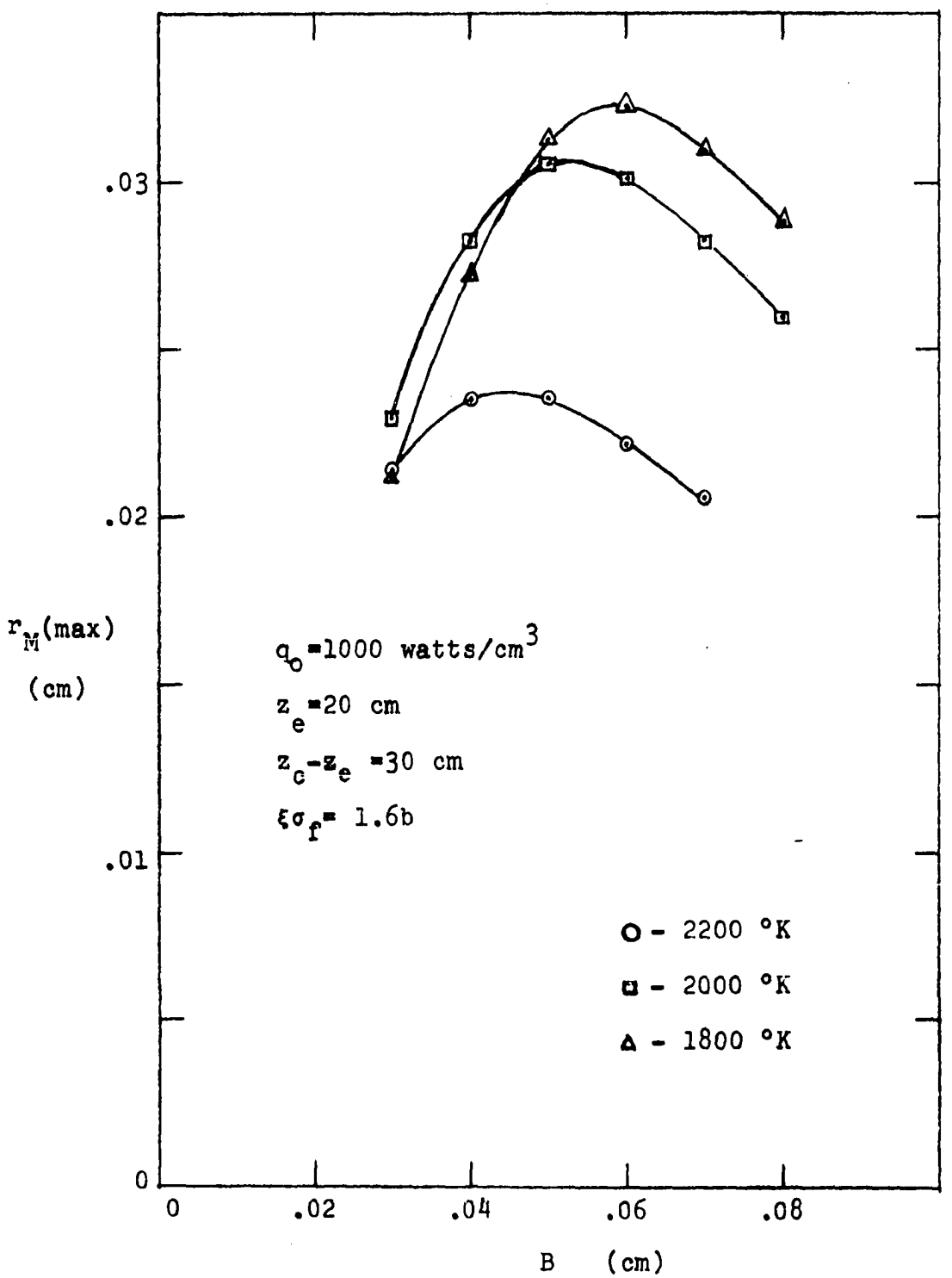

Figure 8. Maximum meniscus radius vs. wick thickness

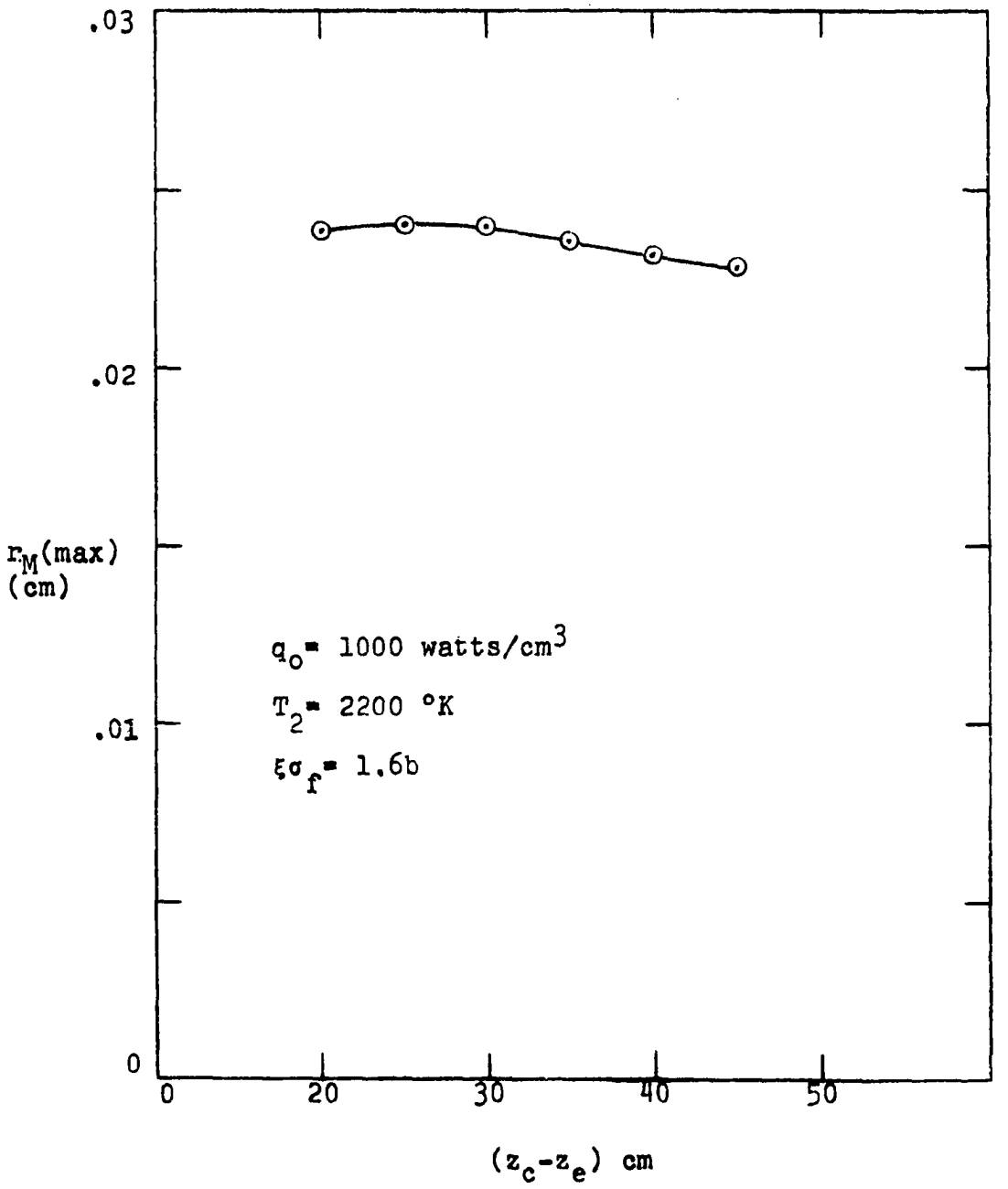

Figure 9. Maximum meniscus radius vs. condenser length

30 cm respectively. A plot of $r_M(max)$, ΔM, and δ vs. Z_e is shown in Figure 10. The value of δ for this graph was evaluated such that $\delta = 0$ when $\Delta M = 0$. The choice of 20 cm is rather arbitrary and takes into account the total volume that many heat pipes would take out of the reactor.

The value of $\xi\sigma_f{}^{235}$ is made as large as possible without causing the heat pipe to fail. An arbitrary limit was set such that $\xi\sigma_f{}^{235}$ was small enough that a 10% increase above design conditions in either flux or temperature would not cause burnout. This point is very hard to determine because burnout was defined as the point where $r_M(max) = r_s$ and r_M approaches r_s in an asymptotic manner although it will reach r_s and become smaller.

After all these variables are determined, the reactivity introduced by a change in flux can be determined. Figure 11 is a plot of $\delta/\Delta\phi/\phi$ vs. ϕ with temperature T_2 as a parameter. The temperature T_2 is constant for each curve although for the real case any change in flux would cause a change in T_2. The value of $\xi\sigma_f{}^{235}$ is 1.6 barns for this plot. Figure 12 is the same as Figure 11 except $\xi\sigma_f{}^{235}$ is increased to 1.75 barns. In this latter case little increase in design temperature or flux can be made without loss of evaporator fluid.

It can be noted from both graphs that for a given flux value, the reactivity caused by a flux change decreases

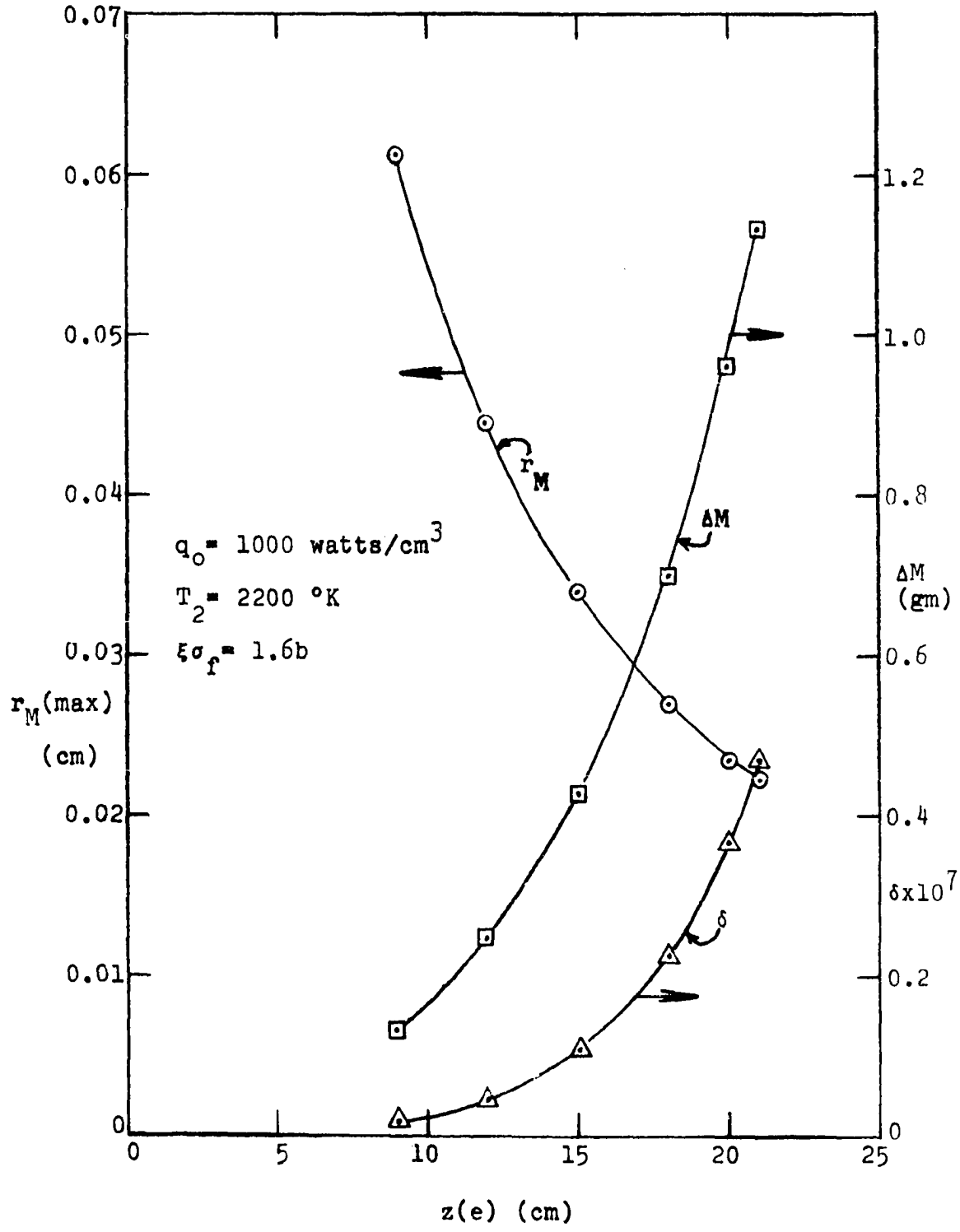

Figure 10. Maximum radius of meniscus, total liquid mass change, and reactivity of heat pipe vs. evaporator length

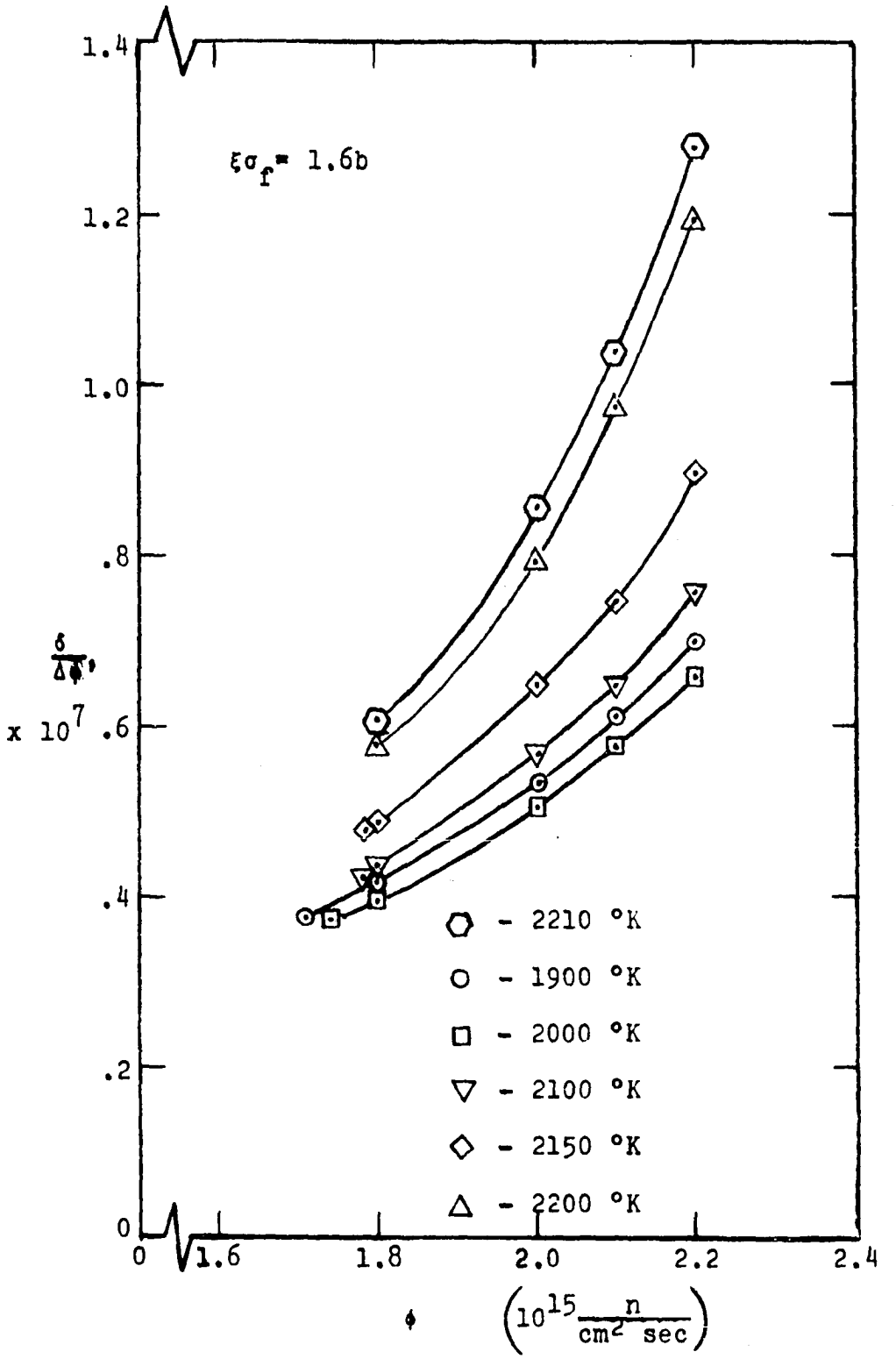

Figure 11. Flux dependent reactivity of heat pipe

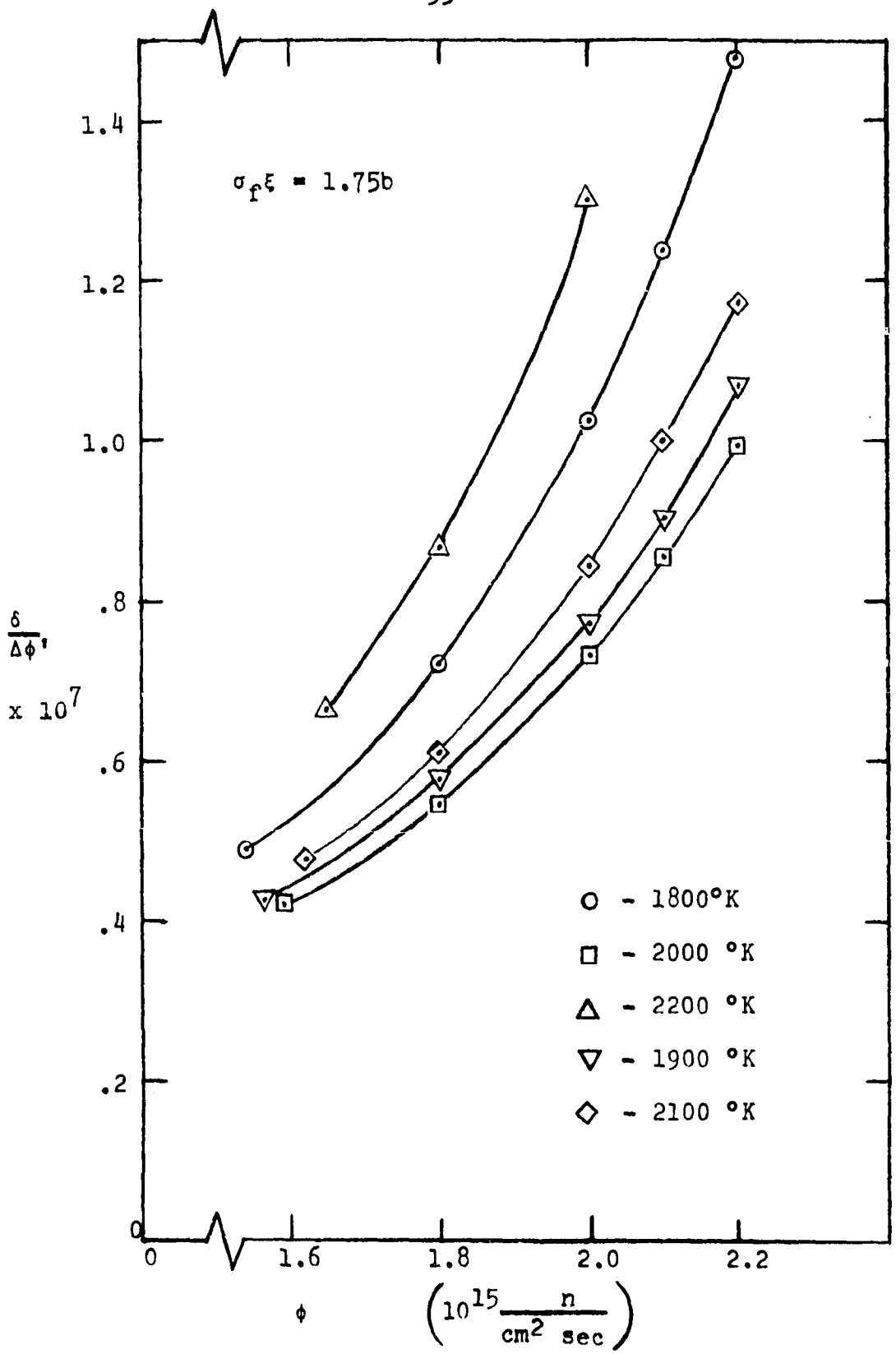

Figure 12. Flux dependent reactivity of heat pipe

initially with temperature and then increases. This phenomenon can be seen more clearly on Figure 13, where δ is plotted against temperature with δ assumed to be zero at T_2 = 2200°K and $\phi = 2\text{x}10^{15} \frac{n}{cm^2 sec}$.

It appears from Figure 13 and 14 that the effect due to change in flux at a constant temperature can be combined in an additive manner with the change in flux at a constant temperature to give the combined effect on reactivity due to both flux and temperature changes for temperatures above 2000°K.

By a trial and error method, the following equation was found to closely approximate the reactivity change due to flux changes and resulting temperature changes for the case of $\xi\sigma_f^{235} = 1.6b$.

$$\frac{\Delta k}{\beta k} = \delta'_{HP} = 4.666\text{x}10^{-5}\Delta T_2' + 91.48\text{x}10^{-5}(\Delta T')^2 + 1.581\text{x}10^{-5} + 4.944\text{x}10^{-5}(\Delta\phi')^2 + 9.04\text{x}10^{-5}(\Delta\phi')^3 \qquad (92)$$

where $\beta = 0.005$.

If the effective number of heat pipes in the reactor is $n\text{x}10^3$, the reactivity due to the heat pipes can be written as

$$\delta'_{HP} = 0.01n\left[4.666\Delta T_2' + 91.48(\Delta T_2')^2 + 1.581\Delta Q' + 4.944(\Delta Q')^2 + 9.04(\Delta Q')^3\right] \qquad (93)$$

where $\Delta T_2' = 1 + T_2'$ and $\Delta Q' = 1 + Q'$. This term equals $f(Q', T_2')$ in Equation 91 and is used there to get the changes

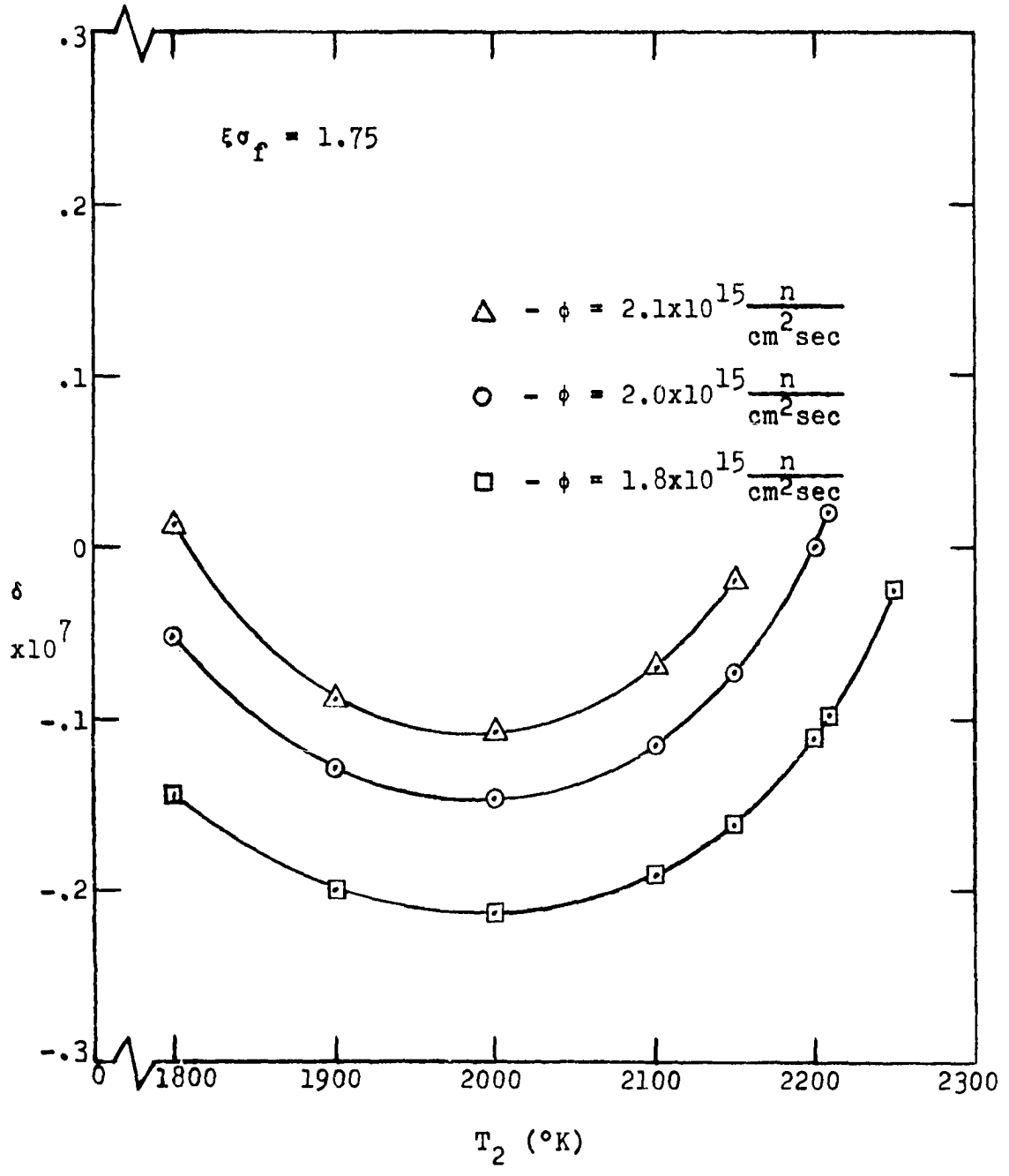

Figure 13. Temperature dependent reactivity of heat pipe

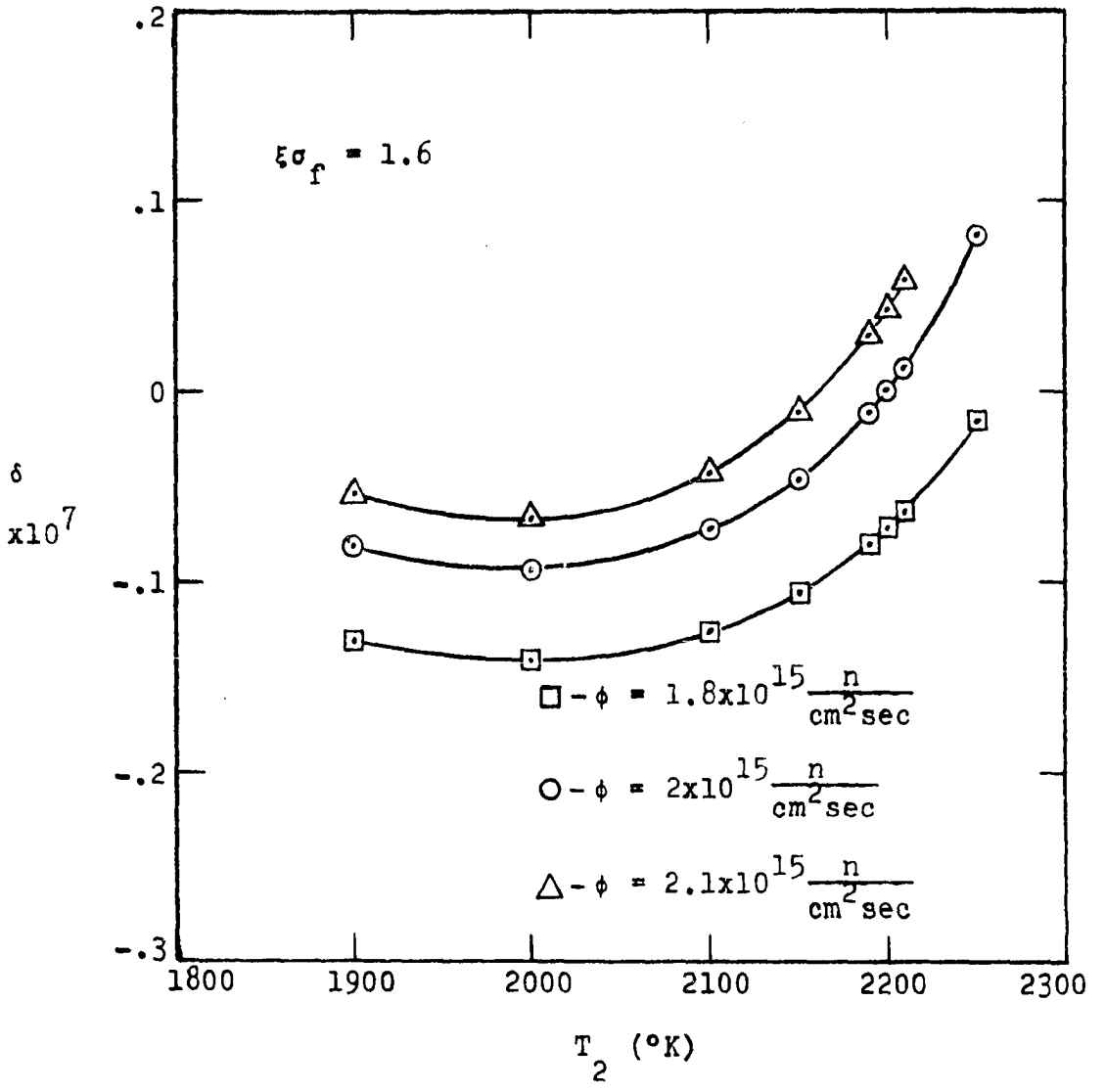

Figure 14. Temperature dependent reactivity of heat pipe

in neutron density with time for changes in reactivity.

Equations 86 through 91 are now solved using an analog computer, these equations are written in terms of changes in the variables from steady state values. Some of the terms have to be written in terms of series expansions and when this is necessary the third order terms and larger are neglected. The only cubic term which will be included is $(\Delta Q')^3$ in the expression for δ'_{HP} because of its relatively large coefficient. However, it will be seen that even this term could be neglected except for very large $\Delta\phi'$'s.

The following equations are used for the solution of n(t) on the analog computer.

$$\tau_n \frac{d\Delta n'}{dt} = \delta' + \delta'\Delta n' - \Delta n' + \frac{\beta_1}{\beta}\Delta C_1' + \frac{\beta_2}{\beta}\Delta C_2' \tag{94}$$

$$\tau_{c1} \frac{d\Delta C_1'}{dt} = \Delta n' - \Delta C_1' \tag{95}$$

$$\tau_{c2} \frac{d\Delta C_2'}{dt} = \Delta n' - \Delta C_2' \tag{96}$$

$$\tau_T \frac{d\Delta T_2'}{dt} = \Delta n' - \frac{1}{2}\Delta T_2' + \frac{1}{8}\Delta T_2' - \Delta P_1' - \frac{1}{2}\Delta P_1'\,\Delta T_2' \tag{97}$$

$$\tau_P \frac{d\Delta P_1'}{dt} = \Delta T_2' - \frac{1}{2}(\Delta T_2')^2 + \frac{3}{2}\Delta P_1'\Delta T_2' - \Delta P_1' - (\Delta P_1')^2 \tag{98}$$

$$\tau_Q \frac{d\Delta Q'}{dt} = \Delta n' - \Delta Q' \tag{99}$$

$$\delta' = \delta_c' - (\alpha_p + \frac{\alpha_T}{2})\Delta T_2' + (\alpha_H + \frac{\alpha_T}{8})(\Delta T_2')^2 + \alpha_H \Delta P_1'$$

$$- \alpha_H \Delta P_1' \Delta T_2' + \delta_{HP}' \qquad (100)$$

Jansen and Buckner (18) suggest that for this type of rocket reactor, two groups of delay neutrons be used with values of β_1 and β_2 both equal to .0025 and λ_1 and λ_2 equal to .046 sec^{-1} and .742 sec^{-1} respectively. These numbers were used in Equations 94, 95, and 96 along with a neutron lifetime of 5×10^{-4} which gives the following values.

$$\tau_n = \frac{\Lambda}{\beta} = 0.1 \text{ sec}^{-1} \qquad (101)$$

$$\tau_{c_1} = \frac{1}{\lambda_1} = 21.65 \text{ sec}^{-1} \qquad (102)$$

$$\tau_{c2} = \frac{1}{\lambda_2} = 1.348 \text{ sec}^{-1} \qquad (103)$$

$$\frac{\beta_1}{\beta} = \frac{\beta_2}{\beta} = 0.50 \qquad (104)$$

Jansen and Buckner also suggest value of α_p and α_T of 1.5 and 1.0 respectively. Along with the values of $\tau_T = 2.5$sec and $\tau_p = 12.5$ sec, this gives all the constants except τ_Q needed for evaluation of Equations 94 through 100.

The value of τ_Q from Equation 71 is

$$\tau_Q = \frac{(z_c + z_e)\rho_v \pi r_v^2 H_v}{2Q(z_e)}$$

$$= \frac{(50\text{cm})\ (.03674\ \frac{\text{gm}}{\text{cm}^3})\ \pi(.5\text{cm})^2(765\ \frac{\text{watts-sec}}{\text{gm}})}{2(837\ \text{watts})} = 0.660\text{sec} \quad (105)$$

for the design conditions.

Figures 15 through 18 show variations of $\Delta n'$ with time. Each one of these graphs is for δ_c' equal to a step function. This would be an approximation to any fast fluctuation which could be approximated with a step function such as a slug of liquid H_2 entering the reactor or a step increase in P_1.

On each graph, n is used as a parameter where $n = 0$ represents the condition of no heat pipes in the reactor. n is the effective number of heat pipes and $nx10^3$ would be equal to the actual number of heat pipes if each heat pipe had the same contribution to the reactivity as the center one, which was analyzed, did.

In Figure 18, where a very large step is used and $\Delta n'$ reaches a high value, a plot was made without the ΔQ^3 term. For this case there is a slight decrease in flux due to the $(\Delta Q')^3$ term. However, in all the previous graphs, it could be neglected.

The value of τ_Q was increased to 1.2 sec and decreased to 0.2 sec and no change in the plots could be seen.

Figures 19 through 23 show the change in $\Delta n'$ for the case of a ramp function of δ_{HP}'. This would be a more realistic approximation of real behavior. The value of δ_{HP}' is

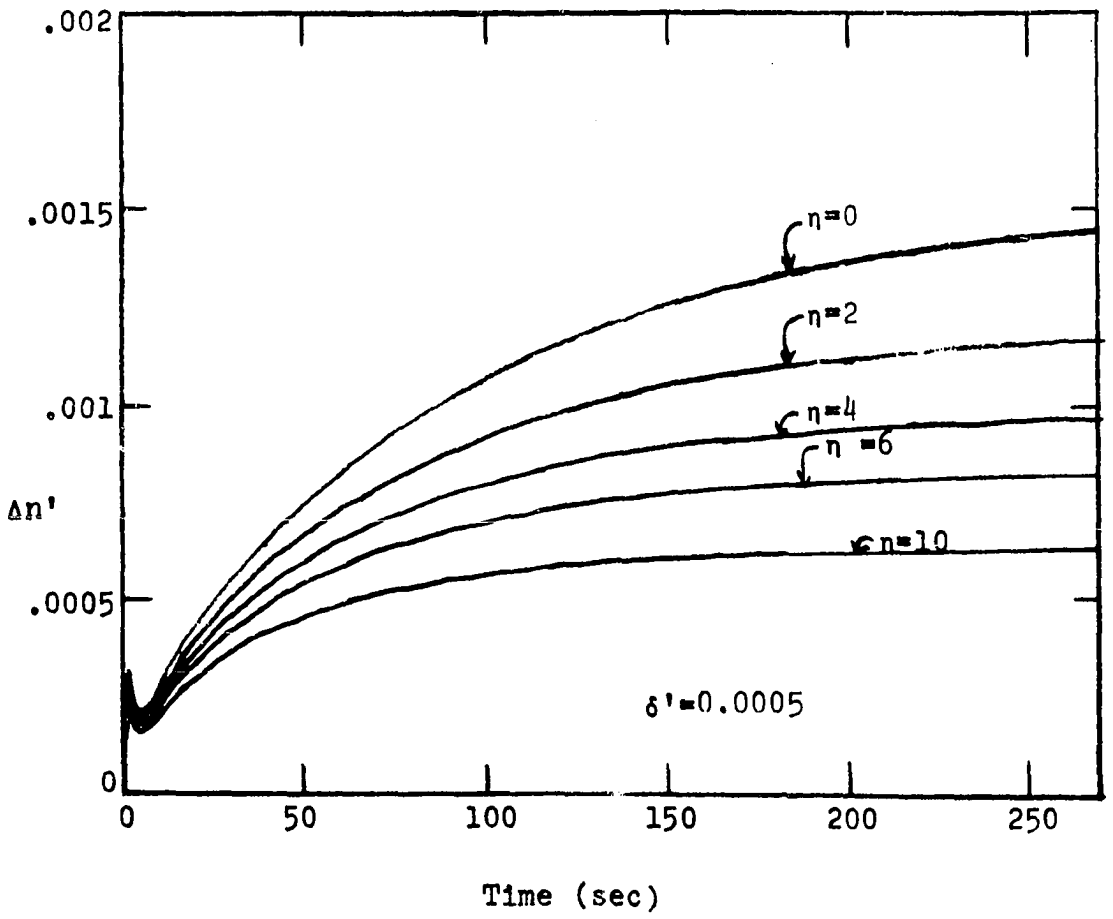

Figure 15. Time dependent neutron density for reactivity equal to step function

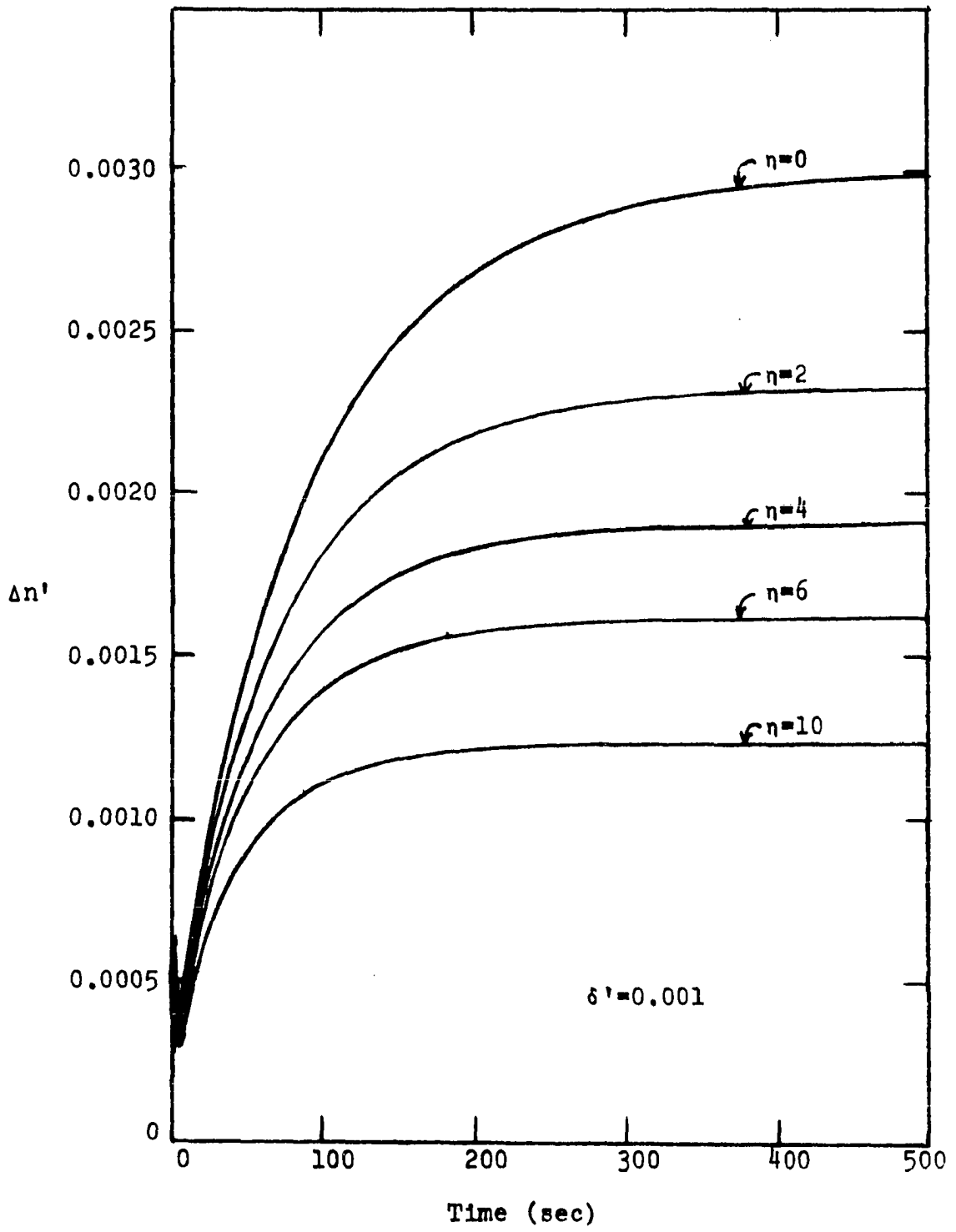

Figure 16. Time dependent neutron density for reactivity equal to step function

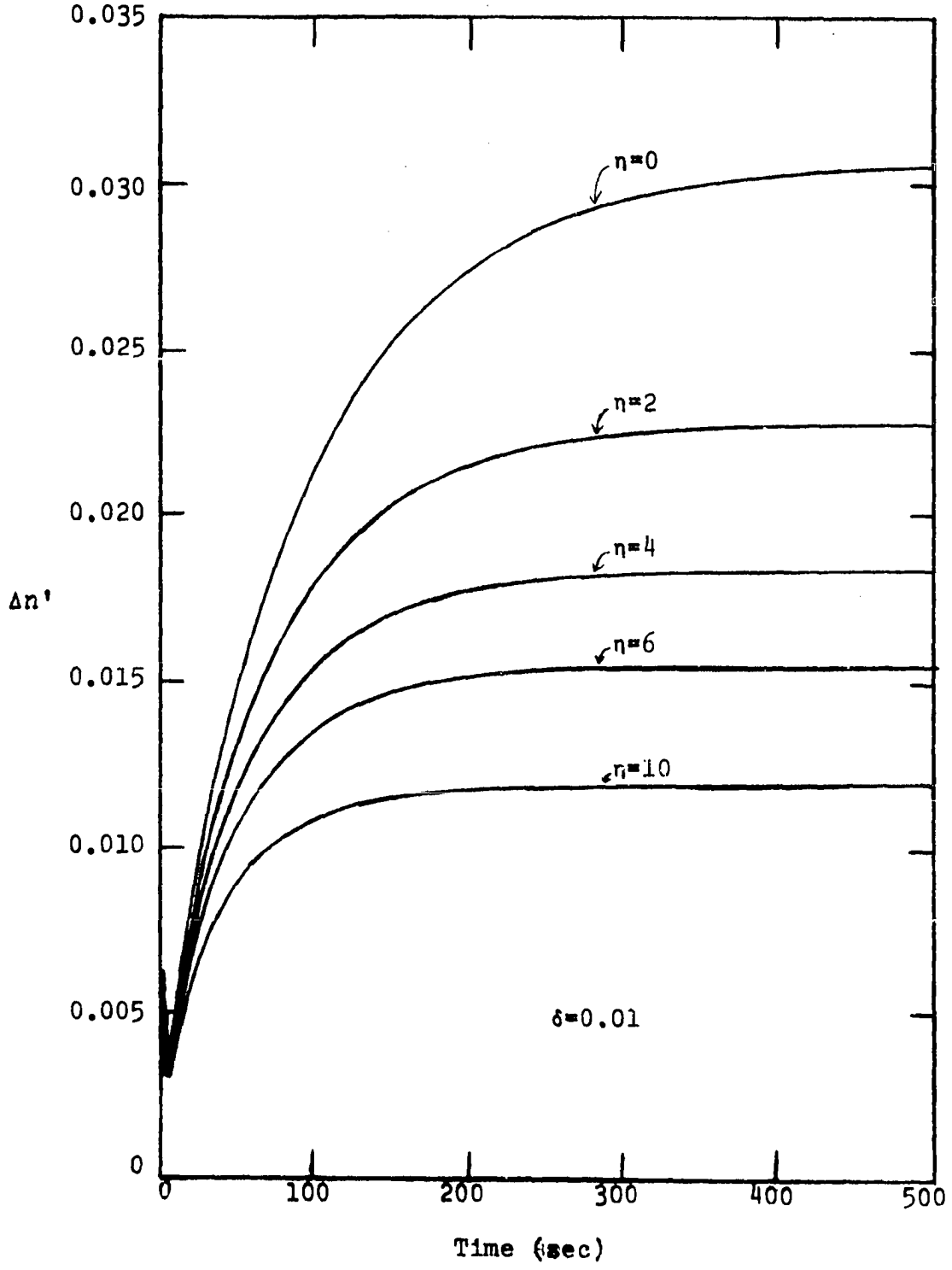

Figure 17. Time dependent neutron density for reactivity equal to step function

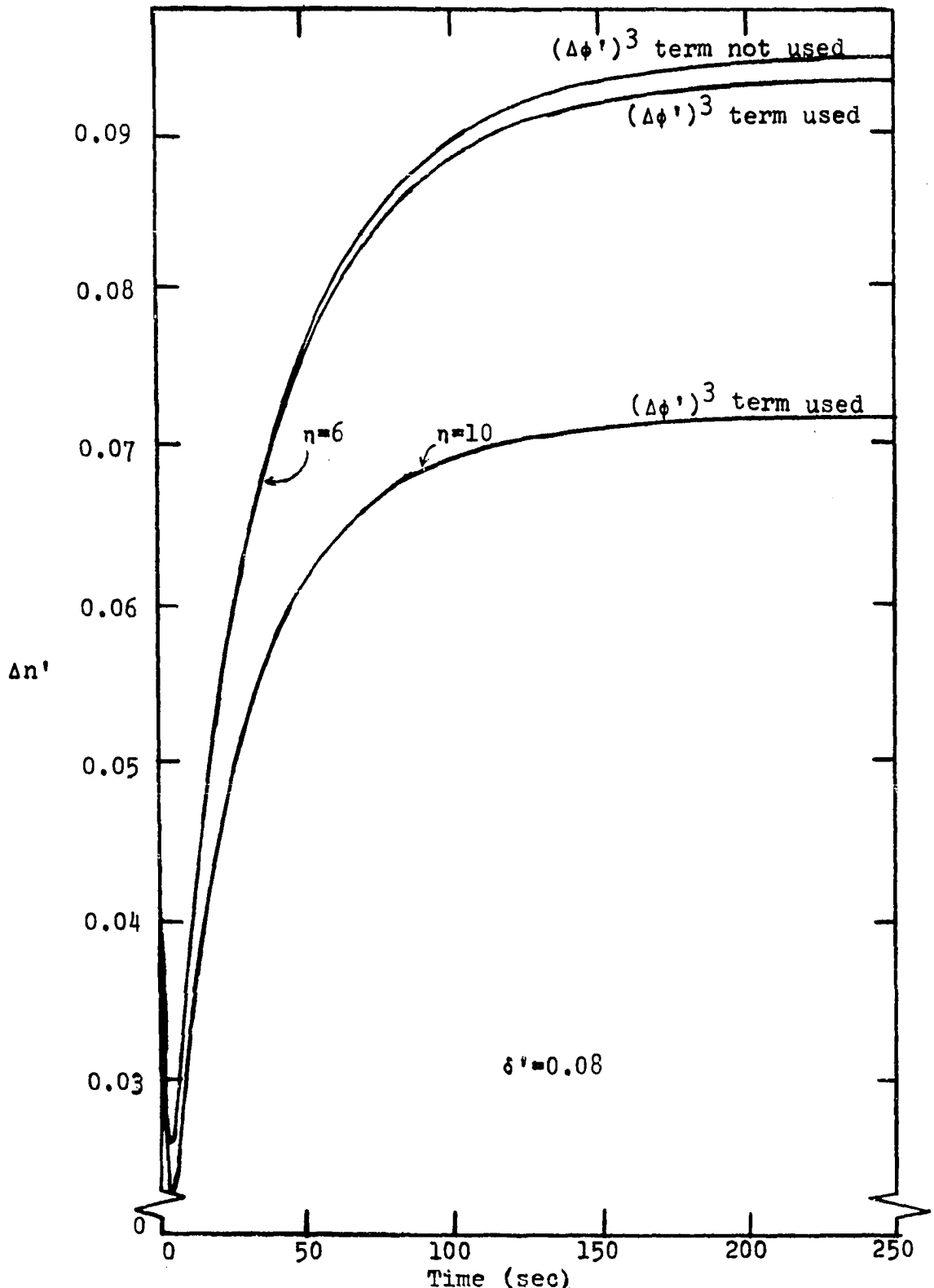

Figure 18. Time dependent neutron density for reactivity equal to step funtion

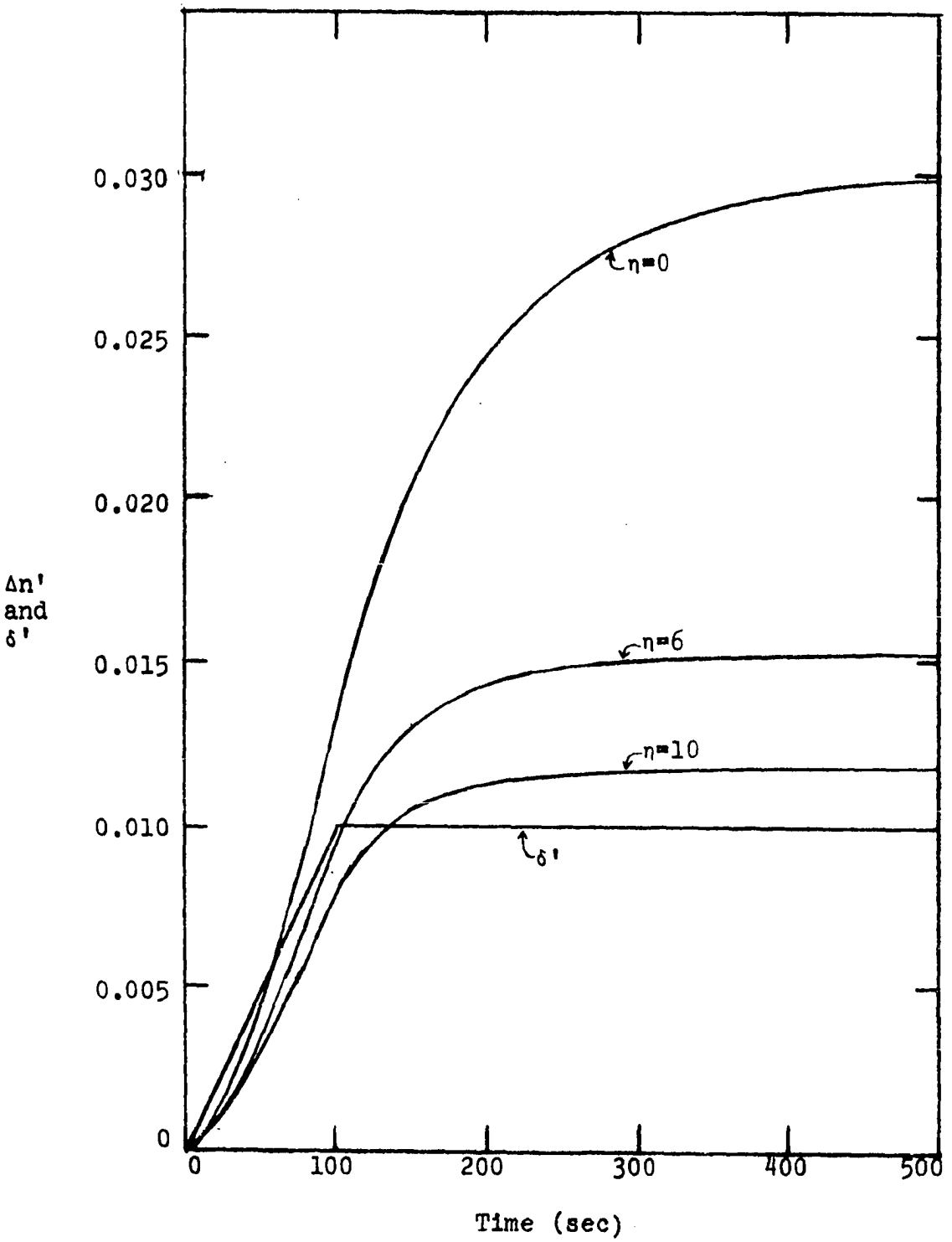

Figure 19. Time dependent neutron density for reactivity equal to ramp function

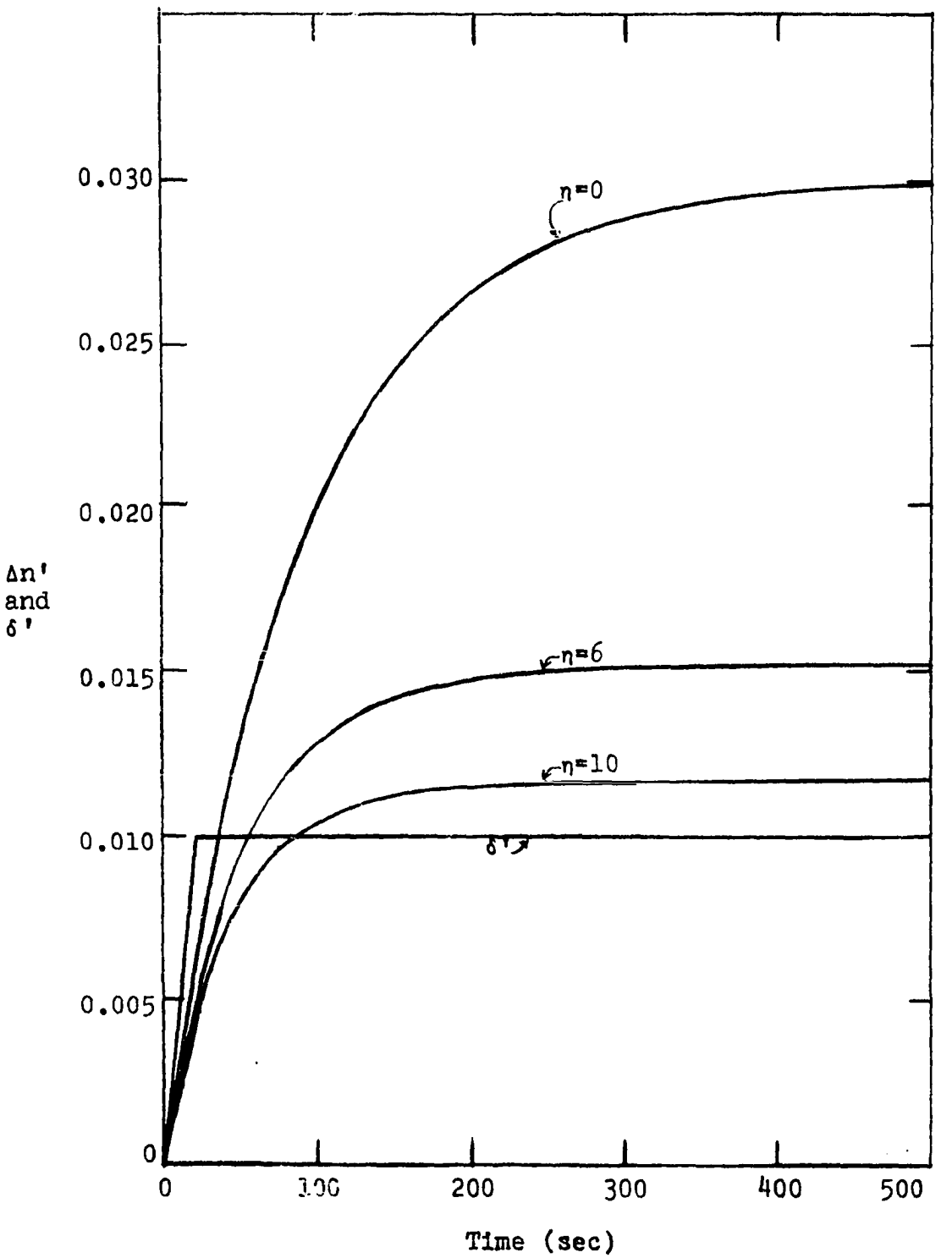

Figure 20. Time dependent neutron density for reactivity equal to ramp function

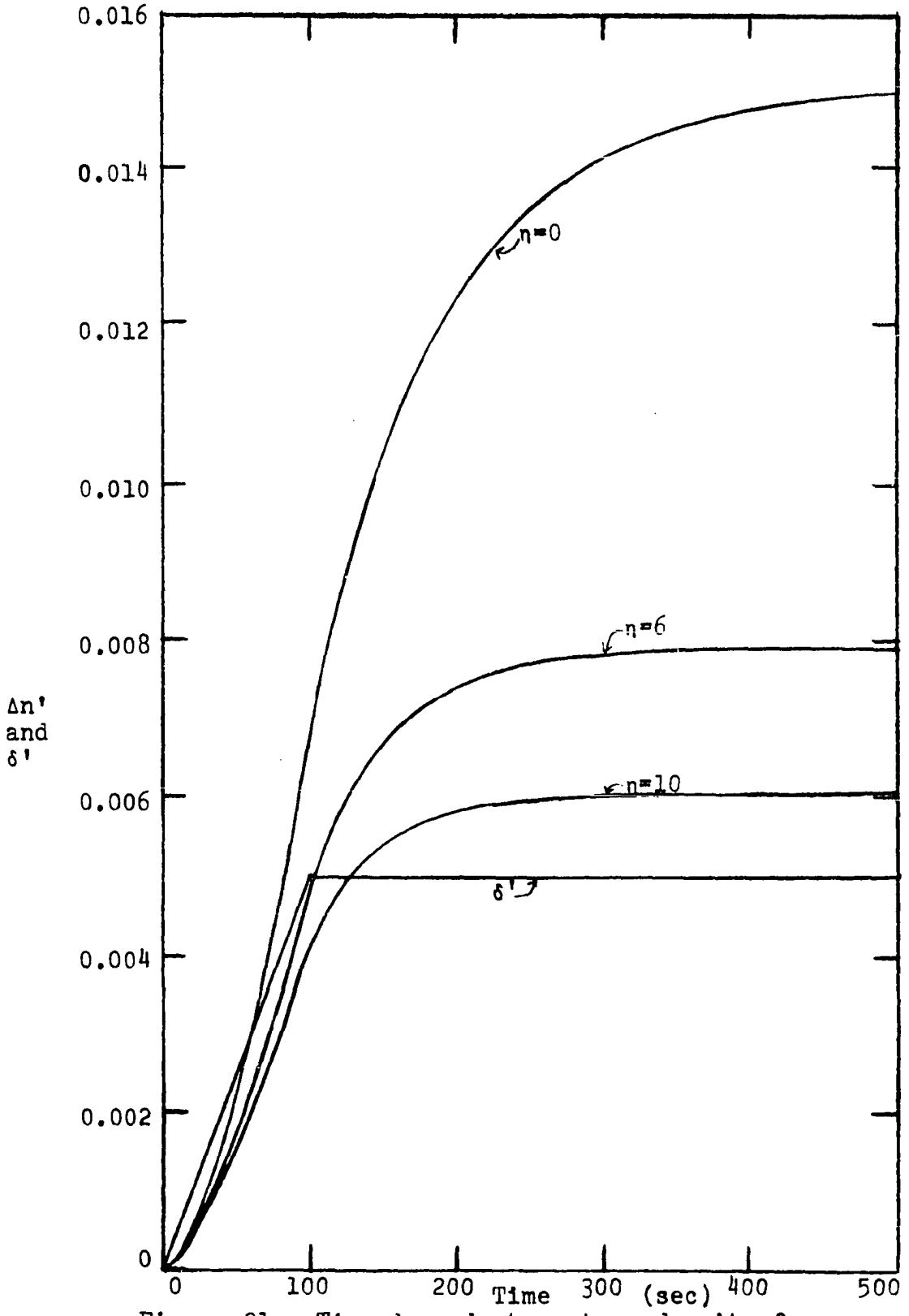

Figure 21. Time dependent neutron density for reactivity equal to ramp function

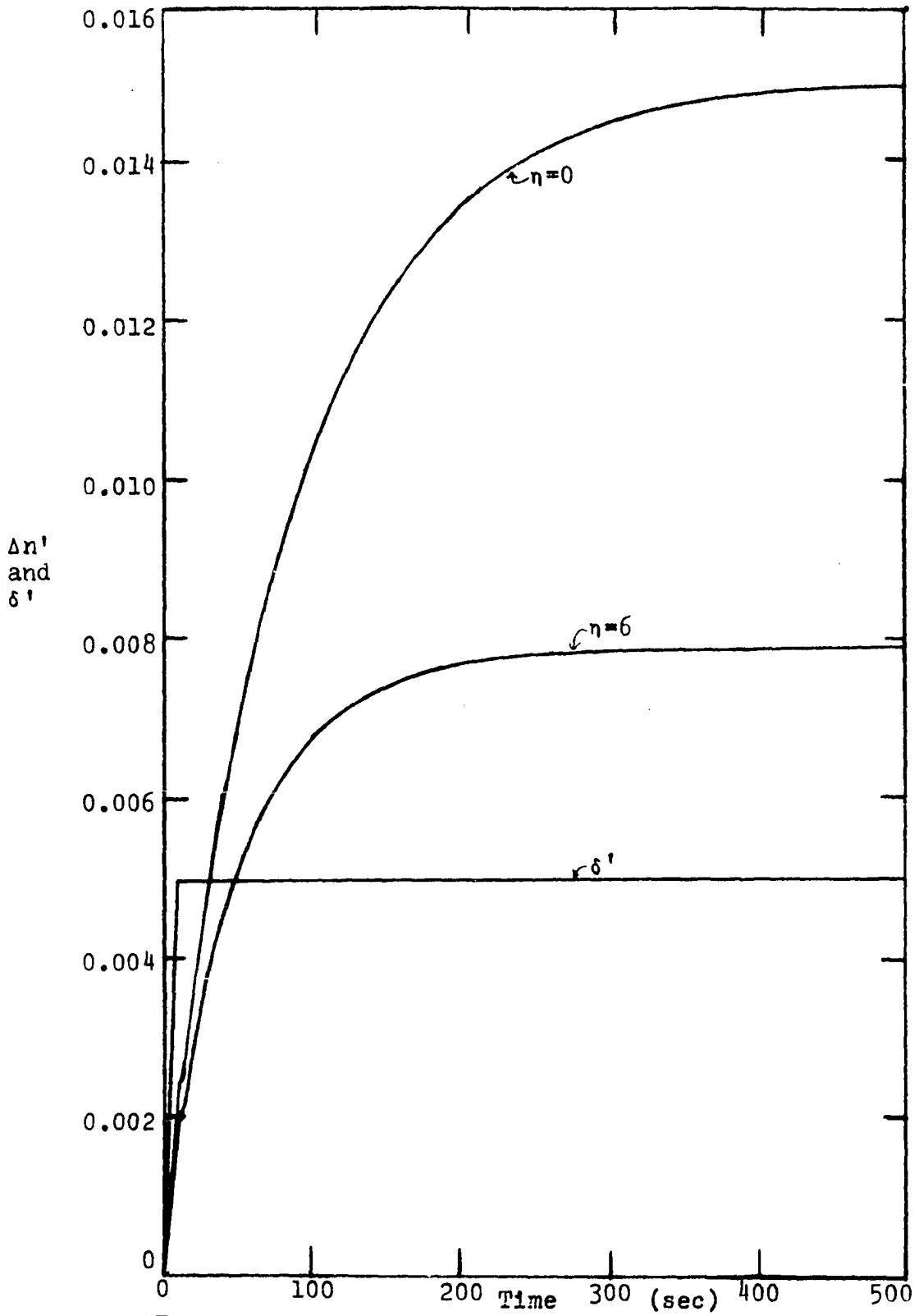

Figure 22. Time dependent neutron density for reactivity equal to ramp function

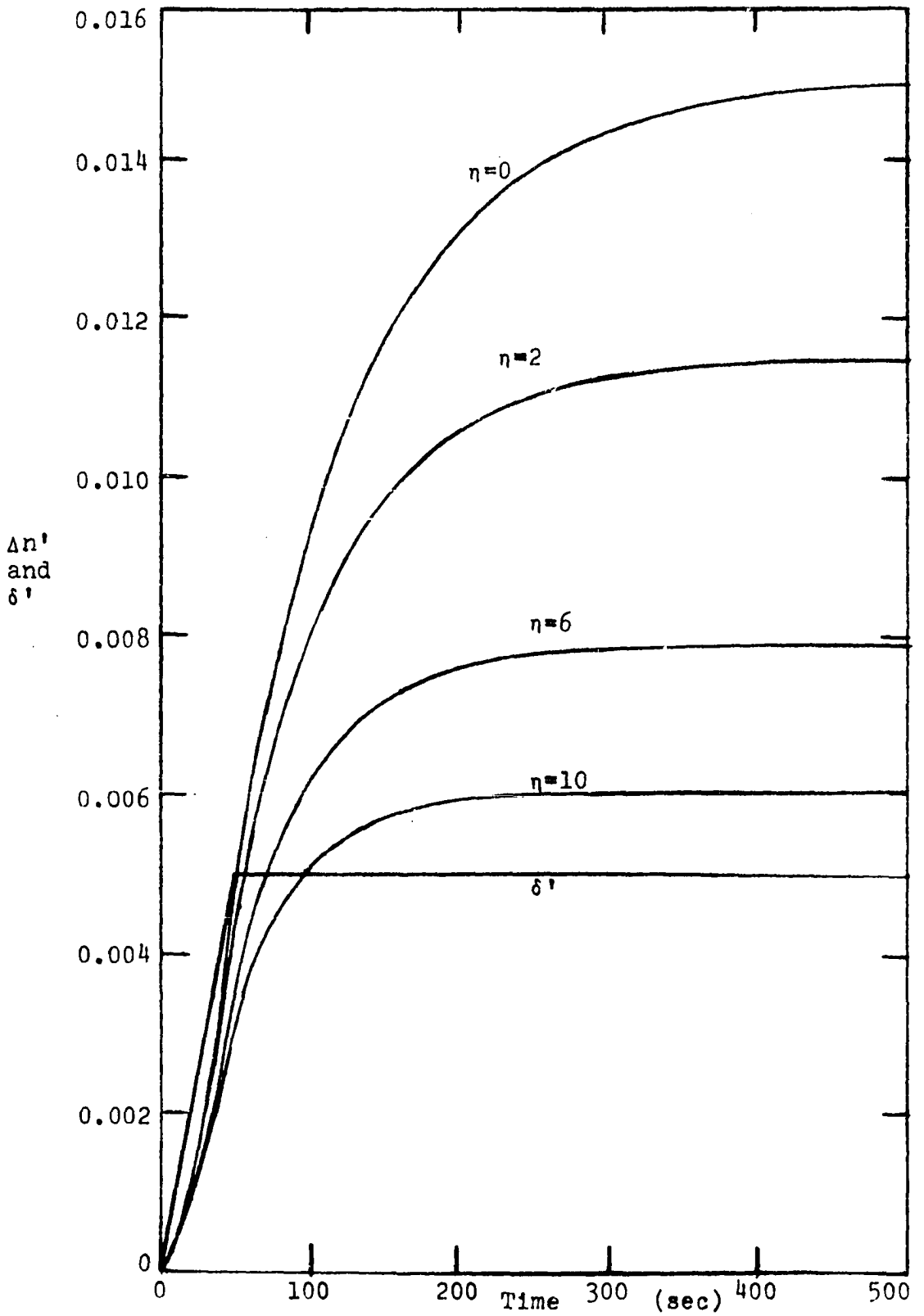

Figure 23. Time dependent neutron density for reactivity equal to ramp function

allowed to increase linearly with time and then hold a constant value as shown on the graphs. The behavior of the $\Delta n'$ is much the same as the step function as far as comparisons between different η values are concerned.

VI. CONCLUSION

It can be seen by looking at Figures 15 through 23 that the heat pipe causes reactivity control on power in the reactor. The heat pipe definitely improves the feedback control and improves it faster the more super critical the reactor becomes. It does have the problem of a non-optimum range of temperature operation.

This fact can be seen by examining Figures 8, 12, and 13. By going to a temperature of 1800°K and a value of B of 0.06 cm., $\xi\sigma^{235}$ could be increased since from Figure 8, $r_M(max)$ is higher for this case. This fact is illustrated in Figure 24 on the following page where $\delta'_{HP}/\Delta Q'$ is plotted against flux for the hypothetical case of a reactor with T_2 equal to 1800°K. $\xi\sigma_f^{235}$ is 2.0 b. For this case at $\phi=2\times10^{15}$, the value of $\delta'_{HP}/\Delta Q'$ is 1.2×10^{-7} which compares with a value of 0.79×10^{-7} from Figure 11 at $T_2=2200°K$.

Another observation which can be made is that a larger reactor would improve the results. An obvious reason for this is that more heat pipes could be used in the larger reactor. A less obvious reason is that for a given power, a larger reactor has a lower power density and a lower flux as seen from Equation 47. The improved effect of a lower power density can be seen by analyzing Equation 49. For the same value of q_o, $\xi\sigma_f^{235}$ is increased because ϕ_o is lowered. With

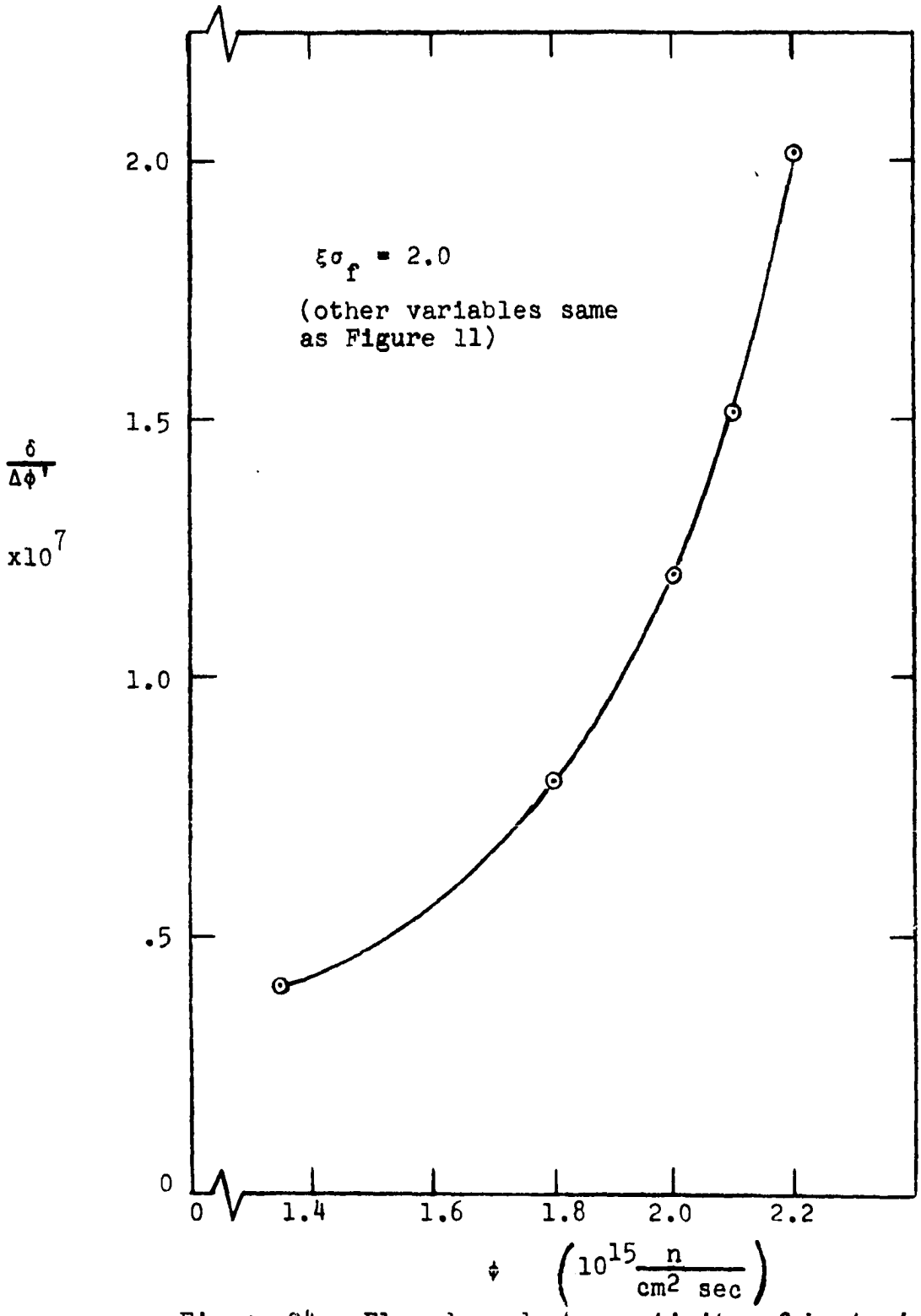

Figure 24. Flux dependent reactivity of heat pipe for T = 1800°K

everything else remaining constant, this would increase C_2 (σ_f, ξ) of Equation 52, and therefore increase the reactivity addition of the heat pipe. An example of the type of reactor where this would be ideal is a very high temperature, large, gas cooled reactor used for power production.

Although it may appear that this system would work better in a section of the reactor where the flux were higher, this is not necessarily true. It would increase the integral term of Equation 52 but $C_2\ (\xi, \sigma_f)^{235}$ could not be made as large because of the power density effect mentioned above.

In summary, it appears that the overall concept is a good method of increasing reactivity feedback if a heat pipe working fluid is used which has optimum temperature operation that matches the operating temperature of the reactor, and that it is better for larger reactors.

VII. SUGGESTIONS FOR FUTURE STUDY

There are numerous applications of this type of heat pipe on which further study could be done. Experimental studies, where facilities permit, are especially needed. A few suggestions for both experimental and analytical work are listed here.

One of the areas where experimental work is needed is in the area of high temperature properties of compounds of fissionable material. More data is needed on the uranium, thorium, and plutonium chlorides, bromides, and fluorides. These compounds appear to have the best stability and high temperature properties for this application.

Another possible investigation is the use of this heat pipe in other types of reactors such as liquid metal fast breeder reactors. It should be possible to use a natural uranium compound in this reactor, with the heat pipes in different areas of the reactor such as in reflectors.

One other possible design is to use heat pipes in a fast reactor with all of the fuel in the heat pipes. This could be used as an auxiliary power supply for space travel. The heat pipes could be used as heat sources for thermoelectric or thermionic energy converters.

Finally, it could be speculated that two component heat pipes could be used. These would have two different working

fluids within the heat pipe. One of these fluids would have a slightly higher boiling point than the other and it would stay in the evaporator section while the other fluid stayed in the condenser. The interface of these fluids would move back and forth short distances depending on the heat flux in the heat pipe. If the fluid in the evaporator were a fissionable fuel and the fluid in the condenser a poison, it would conceivably be possible to get very high reactivity changes with flux changes.

VIII. ACKNOWLEDGEMENTS

The author wishes to express his gratitude to Dr. Glenn Murphy who contributed much appreciated advice and encouragement throughout his college career.

A debt of gratitude is also due to the United States Atomic Energy Commission, who through the Oak Ridge Associated Universities, awarded an AEC Special Fellowship.

The author also wishes to express special thanks to his wife, Lynn, for her understanding and encouragement and for the typing of this thesis.

IX. NOMENCLATURE

Symbol	Term	Dimensions*
B	Annular liquid channel width	L
c_p	Specific heat	$HM^{-1}\theta^{-1}$
d	Diameter	L
g	Acceleration of gravity	LT^{-2}
G	Flow rate per unit area of H_2	$MT^{-1}L^{-2}$
h	Film coefficient	$H\theta^{-1}T^{-1}L^{-2}$
H_v	Heat of vaporization	HM^{-1}
k	Thermal conductivity	$H\theta^{-1}T^{-1}L^{-1}$
m	Mass	M
$\dot{m}$	Mass flow rate	MT^{-1}
$\overline{M}$	Molecular weight	M
M	Mass of liquid displaced by meniscii	M
n	Neutron density	L^{-3}
Na	Avogadro's Number	
p	Pressure	$ML^{-1}T^{-2}$
P	Power	ML^2T^{-3}
Pr	Prandtl Number	
P_e	Pressure drop due to evaporation or condensation	$ML^{-1}T^{-2}$
P_M	Pressure drop due to surface tension effects	$ML^{-1}T^{-2}$

* For the dimensions, L = length, H = heat, M = mass, T = time, and θ = temperature.

q''	Heat flux	$HL^{-2}T^{-1}$
q'''	Heat flux density	$HL^{-3}T^{-1}$
Q	Heat flow rate	HT^{-1}
r	Radius	L
R	Gas constant	$L^{2}T^{-2}\theta^{-1}$
Re	Reynold Number	
T	Temperature	θ
v	Velocity	LT^{-1}
V	Volume	L^{3}
z	Length coordinate along heat pipe axis	L
z_b	Length from point of maximum flux to heat pipe	L
z_e	Length from point of maximum flux to point where flux is zero	L
α	Feedback proportionality constant	
β	Delay neutron fraction	
γ	Surface tension	MT^{-2}
δ	Reactivity	
η	Effective number of heat pipes	
θ	Angle heat pipe makes with horizontal plane	
λ	Precursor decay constant	T^{-1}
Λ	Neutron generation	T
μ	Viscosity	$ML^{-1}T^{-1}$
ν	Number neutrons produced per fission	
ξ	Enrichment	

ρ	Density	ML^{-3}
σ	Microscopic cross-section	L^{-2}
$\delta\Sigma_f$	Change in macroscopic fission cross-section	L^{-1}
$\delta\Sigma_a$	Change in macroscopic absorption cross-section	L^{-1}
τ	Time constant	T
ϕ	Neutron flux	$L^{-2}T^{-1}$
ω	Total mass flow rate of H_2	MT^{-1}

Subscripts

c	Condenser
e	Evaporator
G	Graphite
h	Hydrogen
l	Liquid phase
M	Meniscus
r	Reactor
s	Screen opening
v	Vapor phase
w	Outside wall of heat pipe
1	Reactor entrance plenum
2	Reactor exit chamber

Superscript

'	Variable divided by its design value
d	Design value of variable

X. LITERATURE CITED

1. Anand, D. K. On the performance of a heat pipe. Journal of Spacecraft and Rockets 3, No. 5: 763-765. 1966.

2. Anderson, J. L. and Lantz, E. A nuclear thermionic space power concept using rod control and heat pipes. Nuclear Applications 5, No. 6: 424-436. 1968.

3. Bird, R. B., Stewart, W. E. and Lightfoot, E. N. Transport phenomena. New York, N.Y., John Wiley and Sons, Inc. 1960.

4. Bussard, R. W. and DeLauer. Fundamentals of nuclear flight. New York, N.Y., McGraw-Hill Book Co., Inc. 1965.

5. Carnesale, A., Cosgrove, J. H. and Ferrill, J. K. Operating limits of the heat pipe. U.S. Atomic Energy Report SC-M-66-623 (Sandia Laboratories, Albuquerque, New Mexico) 1966.

6. Cheung, H. A critical review of heat pipe theory and applications. U.S. Atomic Energy Commission Report UCRL-50453 (Lawrence Radiation Laboratory, University of California, Livermore, California) 1968.

7. Cooper, R. S. Nuclear propulsion for space vehicles. Annual Review of Nuclear Science 18: 203-228. 1968.

8. Cotter, T. P. Heat pipe startup dynamics. U.S. Atomic Energy Commission Report LA-DC-9026 (Los Alamos Scientific Laboratory, Los Alamos, New Mexico) 1967.

9. Cotter, T. P. Theory of heat pipes. U.S. Atomic Energy Commission Report LA-3246-MC (Los Alamos Scientific Laboratory, Los Alamos, New Mexico) 1965.

10. Cotter, T. P., Deverall, J., Erickson, G. F., Grover, G. M., Keddy, E. S., Kemme, J. E. and Salmi, E. W. Status report on theory and experiments on heat pipes at Los Alamos. U.S. Atomic Energy Commission Report LA-DC-7206 (Los Alamos Scientific Laboratory, Los Alamos, New Mexico) 1965.

11. Croke, E. J. and Roberts, J. J. Compact power concept features a fast reactor, heat pipes, and direct converters. Reactor and Fuel-Processing Technology 11, No. 4: 187-200. 1968.

12. Deverall, J. E. and Kemme, J. E. Satellite heat pipe. U.S. Atomic Energy Commission Report LA-3278-MC (Los Alamos Scientific Laboratory, Los Alamos, New Mexico) 1965.

13. Feldman, K. T. and Whiting, G. H. Applications of the heat pipe. Mechanical Engineering 90, No. 11: 48-53. 1968.

14. Feldman, K. T. and Whiting, G. H. The heat pipe. Mechanical Engineering 89, No. 2: 30-33. 1967.

15. Grover, G. M., Cotter, T. P., and Erickson, G. F. Structures of very high conductance. Journal of Applied Physics 35: 1990-1991. 1964.

16. Hampel, V. E. and Koopman, R. P. Reactivity self-control on power and temperature in reactors cooled by heat pipes. U.S. Atomic Energy Commission Report UCRL-71198 (Lawrence Radiation Laboratory, University of California, Livermore, California) 1968.

17. Heath, C. A. and Lantz, E. Nuclear thermionic space power system concept employing heat pipes. National Aeronautics and Space Administration Report NASA-TN-D-4299 (Lewis Research Center, Cleveland, Ohio) 1968.

18. Jansen, W. and Buckner, J. K. Starting and control characteristics of nuclear rocket engines. A. I. A. A. Journal 1, No. 3: 563-573. 1963.

19. Kemme, J. E. Heat pipe capability experiments. U.S. Atomic Energy Report LA-3585-MS (Los Alamos Scientific Laboratory, Los Alamos, New Mexico) 1966.

20. Kemme, J. E. Heat pipe design considerations. Unpublished mimeographed paper presented at National Heat Transfer Conference, Minneapolis, Minnesota, August 1969. Los Alamos Scientific Laboratory, Los Alamos, New Mexico. 1969.

21. Kemme, J. E. High performance heat pipes. U.S. Atomic Energy Commission Report LA-DC-9027 (Los Alamos Scientific Laboratory, Los Alamos, New Mexico) 1967.

22. Kirshenbaum, A. D. and Cahill, J. A. The density of molten thorium and uranium tetrafluorides. Journal of Inorganic and Nuclear Chemistry 19, No. 8: 65-68. 1961.

23. Kirshenbaum, A. D. and Grosse, A. V. Basic research in inorganic and physical chemistry at high temperatures. Nuclear Science Abstracts 17, No. 17: 3801. 1963.

24. Knight, B. W. and McInteer, B. B. Laminar incompressible flow in channels with porous walls. U.S. Atomic Energy Commission Report LA-DC-5309 (Los Alamos Scientific Laboratory, Los Alamos, New Mexico) 1957.

25. Lamarsh, J. R. Introduction to nuclear reactor theory. Reading, Massachusetts, Addison-Wesley Publishing Co., Inc. 1966.

26. Langer, S. and Blankenship, F. F. The vapor pressure of uranium tetrafluoride. Journal of Inorganic and Nuclear Chemistry 14, No. 8: 26-31. 1960.

27. Lubarsky, B. and Shure, L. I. Applications of power systems to specific missions. Space Power Systems Advanced Technology Conference NASA-SP-131: 269-277 (National Aeronautics and Space Administration) 1966.

28. Mohler, R. R. and Perry, J. E. Nuclear rocket engine control. Nucleonics 19, No. 4: 80-84. 1961.

29. Moore, W. J. Physical chemistry. 3rd ed. Englewood Cliffs, New Jersey, Prentice-Hall, Inc. 1962.

30. Smith, H. P. Closed loop dynamics of nuclear rocket engines with bleed turbine drive. Nuclear Science and Engineering 14, No. 4: 371-379. 1962.

31. Smith, H. P. and Stenning, A. H. Open loop stability and response of nuclear rocket engines. Nuclear Science and Engineering 11, No. 1: 76-84. 1961.

32. Spence, R. W. The rover nuclear rocket program. Science 160, No. 3831: 953-959. 1968.

33. Standard mathematical tables. 12th ed. Cleveland, Ohio, Chemical Rubber Publishing Company. 1959.

34. Stephenson, M. E. Property values of parahydrogen. U.S. Atomic Energy Commission Report ANL-7004 (Argonne National Laboratory, Argonne, Illinois) 1965.

35. Valfells, A. Preliminary design of a power generating system using a fissile gas. Unpublished Ph.D. thesis. Ames, Iowa, Library, Iowa State University of Science and Technology. 1962.

36. Wageman, W. E. and Guevara, F. A. Fluid flow through a porous channel. Physics of Fluids 3: 878-880. 1960.

37. Wagner, P. and Dauelsberg, L. B. The thermal conductivity of ZTA graphite. Carbon 5, No. 6: 271-279. 1967.

38. Yuan, S. W. and Finkelstein, A. B. Laminar pipe flow with injection and suction through a porous wall. A. S. M. E. Transactions 78: 719-724. 1956.